



**The Abdus Salam
International Centre for Theoretical Physics**



2052-29

Summer College on Plasma Physics

10 - 28 August 2009

**Collective effects of intense ion and electron flows propagating
through background plasma**

Igor D. Kaganovich
*Princeton Plasma Physics Laboratory
Princeton University*

USA

Collective effects of intense ion and electron flows propagating through background plasma

**I. D. Kaganovich, M. A. Dorf,
E. A. Startsev, R. C. Davidson,
A. B. Sefkow, B. C. Lyons, J. S. Pennington**

Princeton Plasma Physics Laboratory, USA

Outline

- **Short overview of collective focusing**
 - Gabor lens
 - Collective (Robertson) lens
 - Passive plasma lenses
- **neutralization of ion beam space charge by a background plasma**
- **collisionless ion heating by an intense electron beam due to development of the Weibel instability**
- **operation of the Hall thruster with intense secondary electron emission**

50 years of collective focusing and acceleration ideas: acceleration (1/2)

- **Acceleration and focusing by a self fields in beams.**

V.I. Veksler, Ya.B. Fainberg, Budker, Proceedings of CERN Symposium on High-Energy Physics, Geneva, 1956.

- **Laser- plasma wake field accelerator,**

Tajima and Dawson, PRL 43, 267 (1979).

- **Beam -plasma wake field accelerator**

P. Chen et al, PRL 54, 693 (1985).

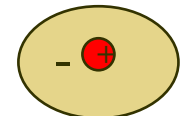
- **Collective ion acceleration by electron beams**

A.A. Plyutto, Sov. Phys. JEPT (1960).

V.I. Veksler, et al Proc. VI Conf. High Energy Accel. (1967). Electron rings

J.R. Uglum and S. Graybill J. Appl. Phys. 41, 236 (1970).

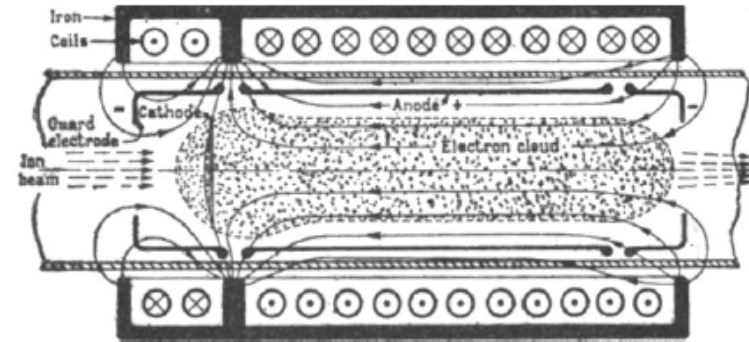
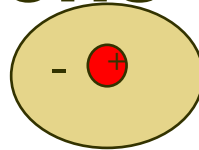
Ions trapped in an electron bunch $v_i = v_e$ energy M/m times.



50 years of collective focusing and acceleration ideas: focusing (2/2)

● Space-charge lens

D. Gabor, Nature 1947

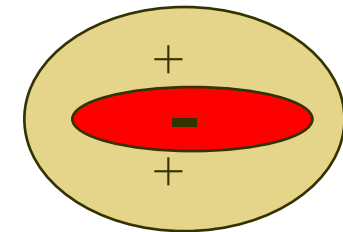


MAGNETRON LENS FOR ION BEAMS

● Underdense plasma lens

P. Chen, Part. Accel. 20 171 (1987).

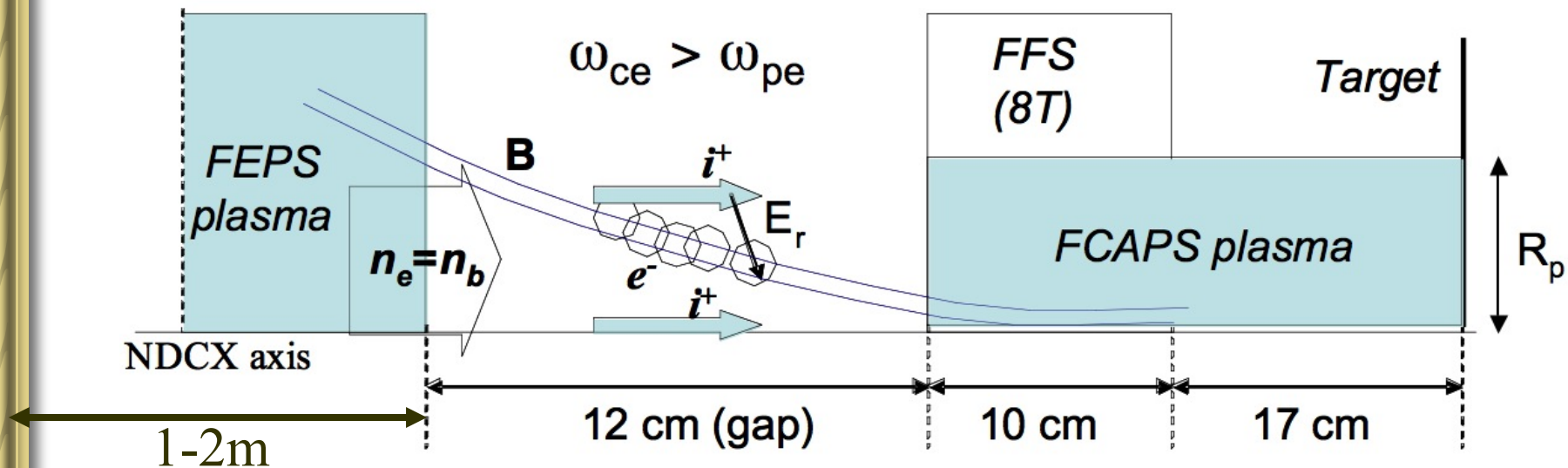
The strong electric field created by the space charge of an electron beam ejects the plasma electrons from the beam region entirely, leaving a uniform ion column.



● Overdense plasma lens

Self-electric field is neutralized. Self-magnetic field is not neutralized.

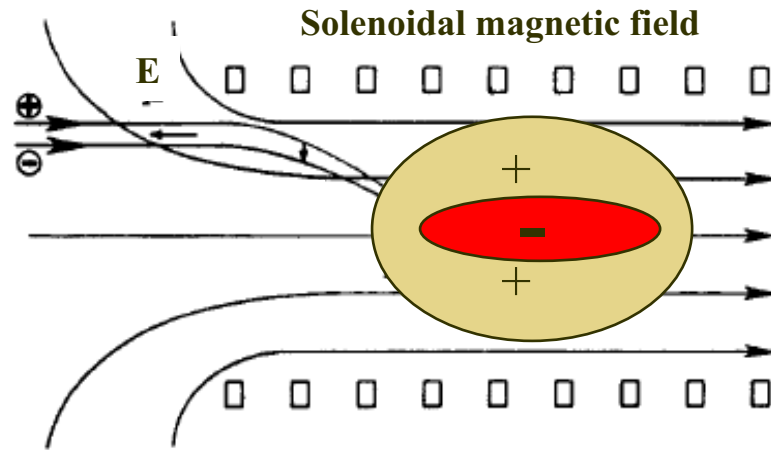
Long neutralized transport in plasma (1-2 m)
 long \Rightarrow focusing effects in plasma are important



- **Generation of large radial electric fields in presence of magnetic field is the most deleterious effect for radial compression.**

Collective Focusing Concept

(S. Robertson 1982, R. Kraft 1987)



From R. Kraft, Phys. Fluids **30**, 245 (1987)

$$\begin{cases} \ddot{r}_e + \frac{1}{4} r_e \Omega_e^2 + \frac{e}{m_e} E_r = 0 \\ \ddot{r}_i + \frac{1}{4} r_i \Omega_i^2 - \frac{e}{m_i} E_r = 0 \end{cases} \quad \text{Quasineutrality} \begin{cases} r_e = r_i \\ \Rightarrow \begin{cases} eE_r = \frac{m_e}{4} r \Omega_e^2 \\ \ddot{r} = \frac{e}{m_i} \frac{m_e}{4} r \Omega_e^2 = \frac{e}{4} r \Omega_e \Omega_i \end{cases} \end{cases}$$

For a given focal length the magnetic field required for a neutralized beam is smaller by a factor of $(m_e/m_i)^{1/2}$.

NDCX-I: $m_i/m_e = 71175$ \longrightarrow **8 T Solenoid can be replaced with 300 G.**

Review of Collective Focusing Experiments

S. Robertson, PRL, **48**, 149 (1982).
Thin collective lens

$E_b \sim 149$ keV, $r_b \sim 15$ cm, $j_b \sim 0.5$ A/cm²,

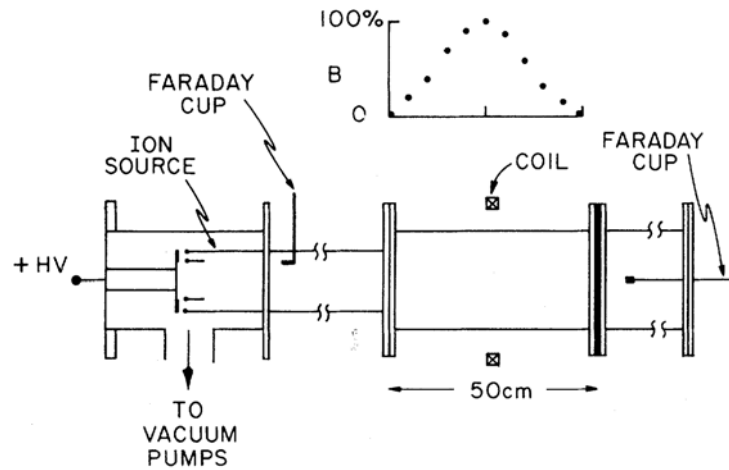


FIG. 1. Schematic diagram of the experimental apparatus.

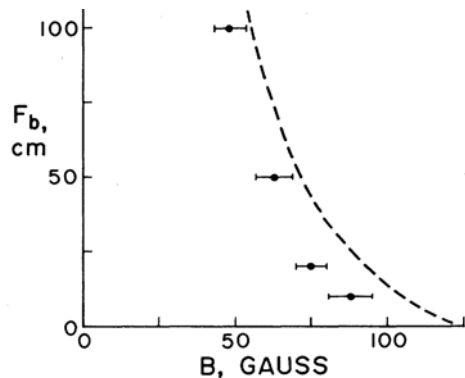


FIG. 4. The experimentally determined focal length as a function of magnetic field (points) and the calculated focal length (dotted line). The error bars give only the statistical uncertainty.

R. Kraft, Phys. Fluids, **30**, 245 (1987).
Thick collective lens

$E_b \sim 360$ keV, $r_b \sim 2$ cm, $n_b \sim 1.5 \cdot 10^{11}$ cm⁻³

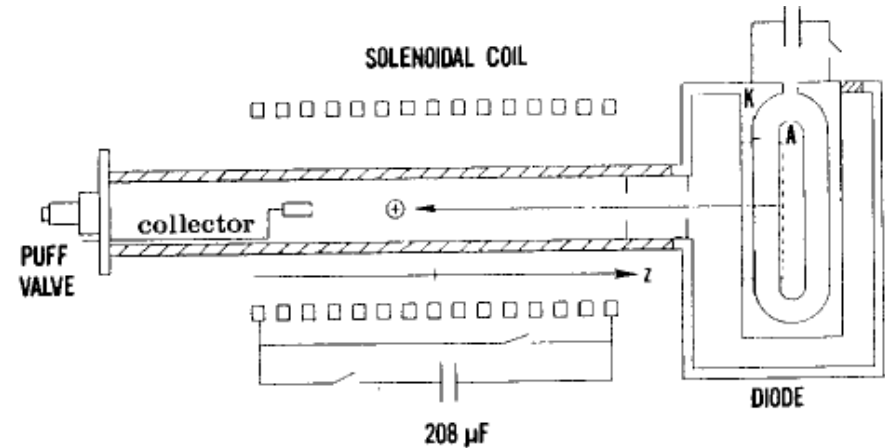


FIG. 1. Experimental apparatus.

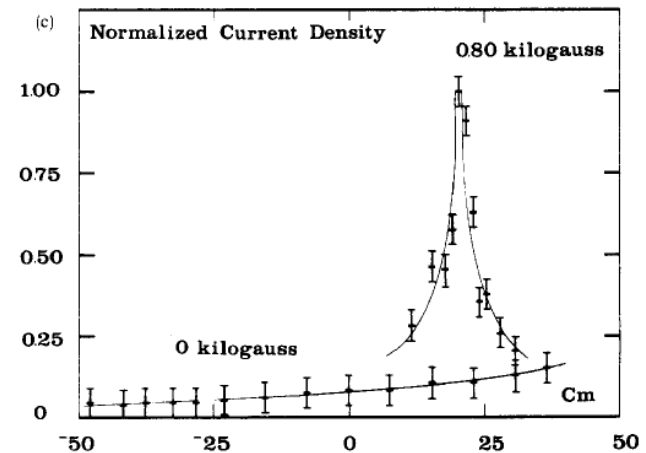


FIG. 8. Focused ion current. (a) Ion current density versus time ($B = 0$, 1.5 kG). (b) Peak ion current density versus axial position ($B = 0$, 1.5 kG). (c) Peak ion current density versus axial position ($B = 0$, 1.5 kG).

Conditions for Collective Focusing

○ $\omega_{pe} \geq \Omega_e / \sqrt{2}$ to maintain quasi-neutrality

$$\left\{ \begin{array}{l} E_r = -\frac{r}{2e} m_e \omega_{pe}^2 \frac{(n_i - n)}{n_e} \quad (\text{Poisson's Eq.}) \\ E_r = -\frac{r}{4e} m_e \Omega_e^2 \end{array} \right.$$

○ $r_b \leq 2c/\omega_{pe}$ to assure small magnetic field perturbations (due to the beam)

$$\left\{ \begin{array}{l} j_\theta = en_e \Omega_e r / 2 \\ \frac{\Delta B_z}{B_0} = \frac{4\pi en_e \Omega_e r_b^2}{c 4B_0} = \frac{\omega_{pe}^2 r_b^2}{4c^2} \end{array} \right.$$

○ Neutralizing electrons have to be dragged through the magnetic field fall-off region to acquire the necessary rotation ($\omega_e = \Omega_e / 2$).

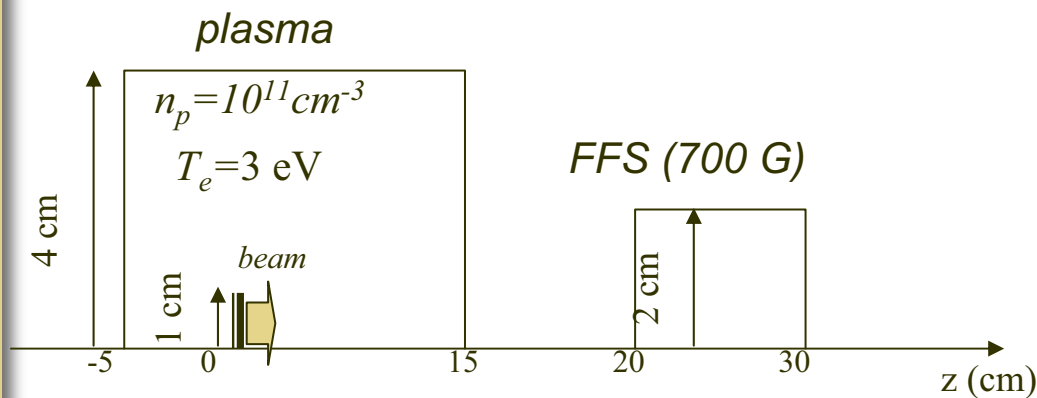


○ Plasma (or secondary electrons) should not be present inside the FFS.

○ Otherwise non-rotating plasma (secondary) electrons will replace rotating electrons (moving with the beam), and enhanced electrostatic focusing will be lost → **FCAPS must be turned off.**

Experimentally verified (R. Kraft 1987)

PIC Simulations show Collective Focusing Lens Can be Used for NDCX Beam Final Focus



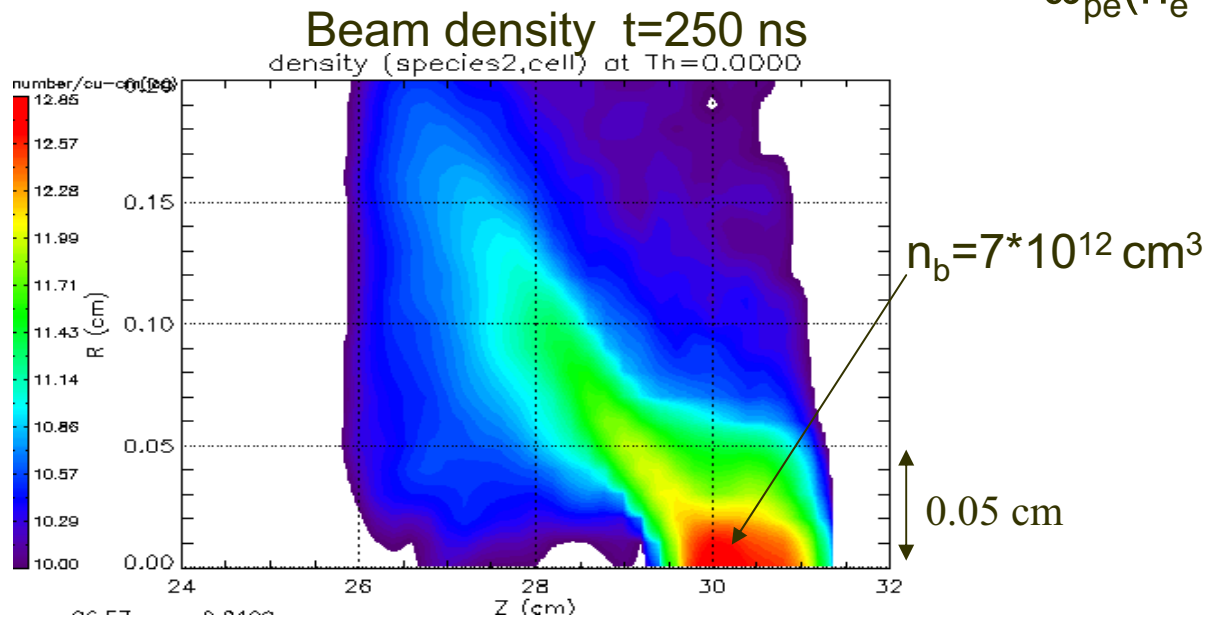
Beam injection parameters

$\text{K}^+ @ 320 \text{ keV}, n_b = 10^{10} \text{ cm}^{-3}$

$r_b = 1 \text{ cm}, T_b = 0.2 \text{ eV}$

beam pulse = 40 ns (5 cm)

$$\omega_{pe}(n_e = n_b) = 0.46 \omega_{ce}$$



Passive plasma lenses

- **Overdense plasma lens, $n_p > n_b$**

Self-electric field is neutralized. Self-magnetic field is not neutralized; $ev_z B_\phi / c$ force focuses beam particles.

Condition: $r_b < 0.5c/\omega_p$; for $n_p = 2.5 \cdot 10^{11} \text{ cm}^{-3}$, $r_b < 5 \text{ mm}$.

Experiments: 3.8 MeV, 25 ps electron beam focused by a $n_p = 2.5 \cdot 10^{11} \text{ cm}^{-3}$ RF plasma

VOLUME 72, NUMBER 15 PHYSICAL REVIEW LETTERS 11 APRIL 1994

Experimental Demonstration of Dynamic Focusing of a Relativistic Electron Bunch by an Overdense Plasma Lens

G. Hairapetian, P. Davis, C. E. Clayton, and C. Joshi
es. Los Angeles, California 90024

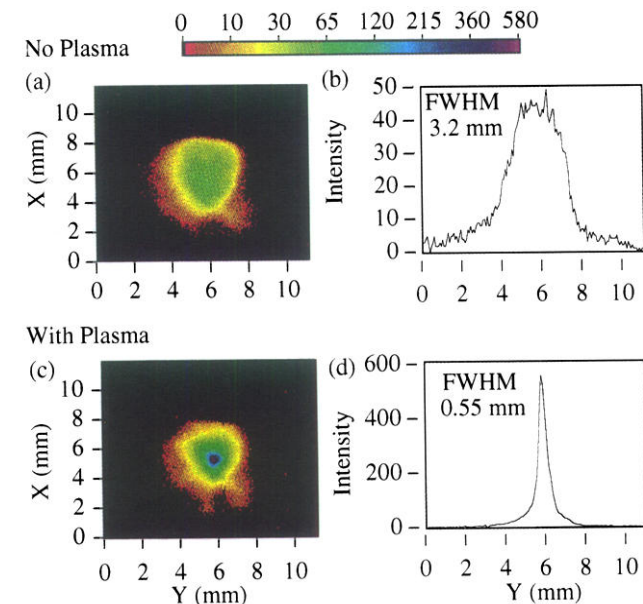
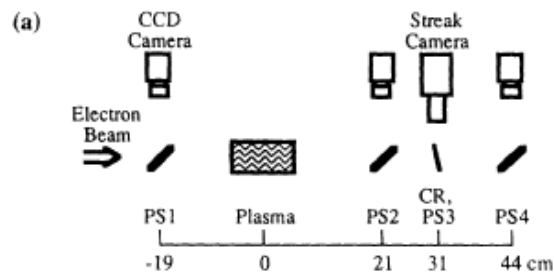
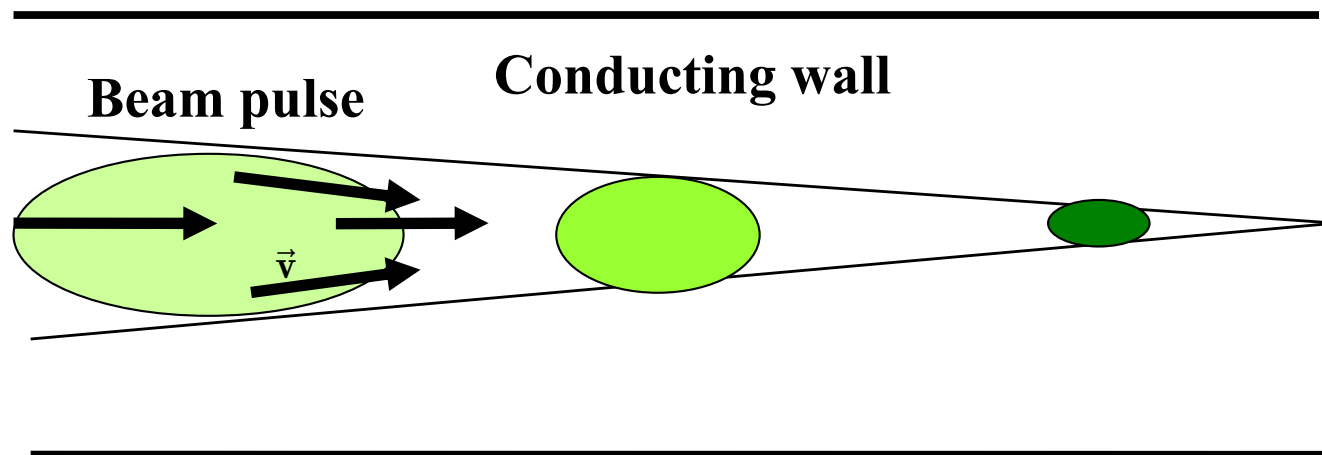


FIG. 3. (a) Time-integrated bunch image with no plasma

The physics of the neutralization process and requirements for plasma sources.

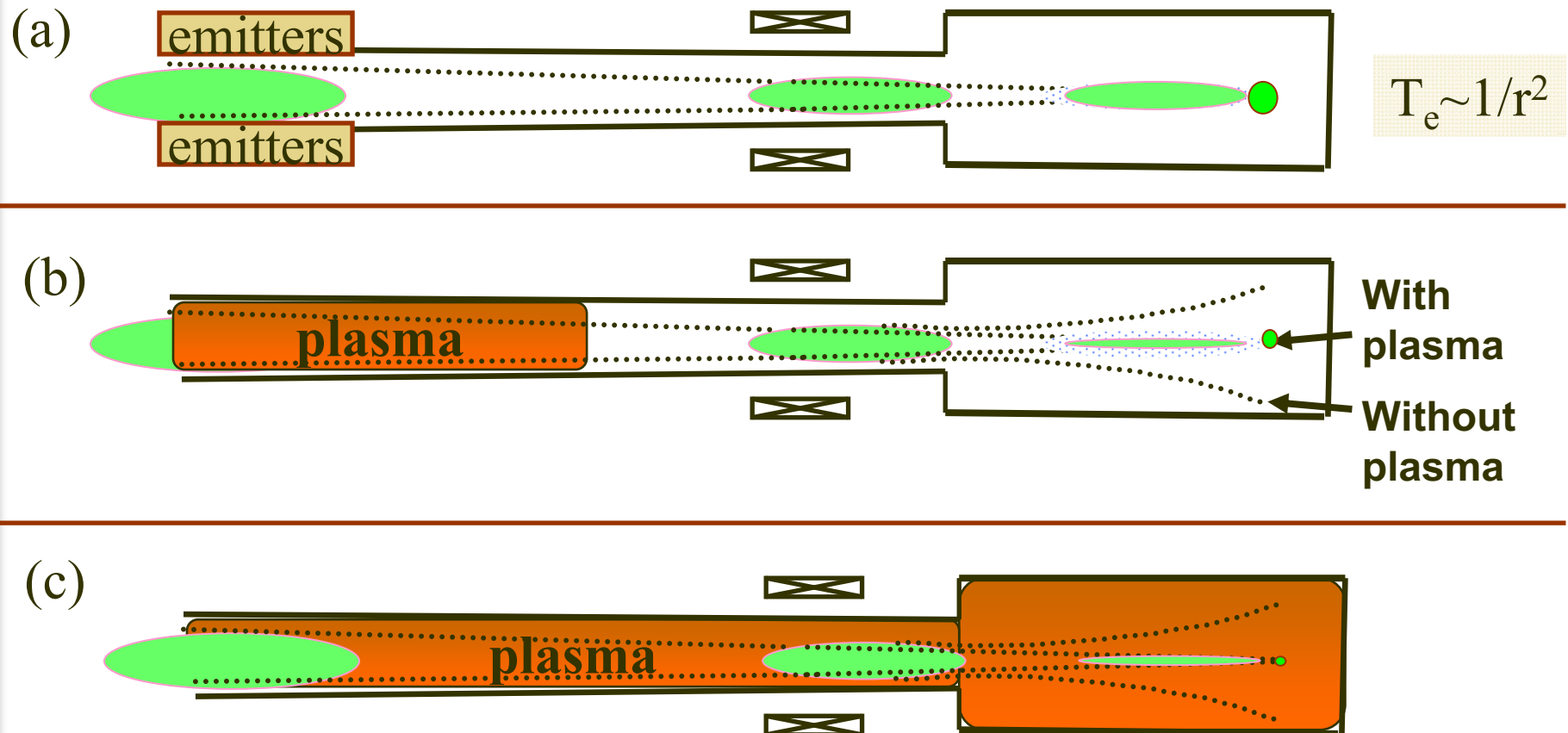
Is it possible to achieve better than 99% neutralization for ion beam focusing during neutralized drift compression?!



Methods to neutralize intense ion beam

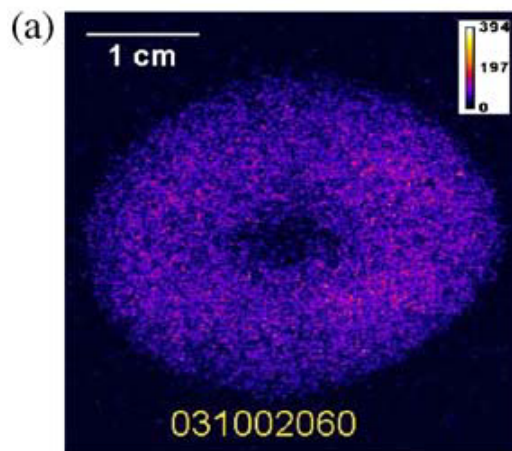
It's better to light a candle than curse the darkness:
It is better to use electrons than fight their presence.

(a) emitters, (b) plasma plug, and (c) plasma everywhere

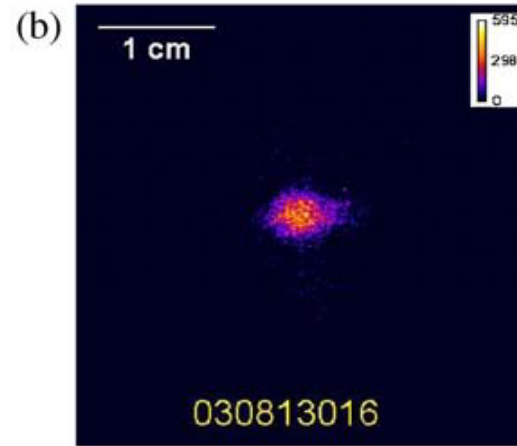


Plasma plug cannot provide sufficient neutralization compared with plasma filling entire volume.

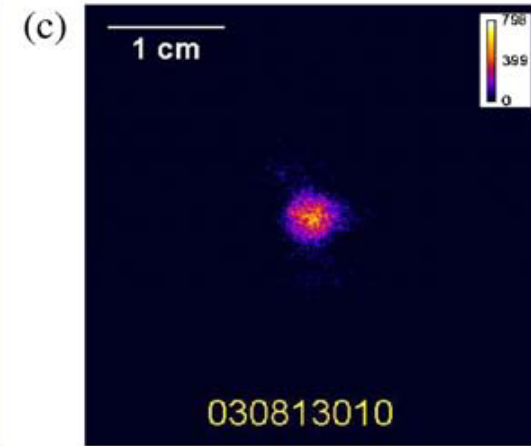
Beam images at the focal plane non-neutralized (a), neutralized plasma plug (b), and volumetric plasma everywhere (c).



FWHM: 2.71 cm

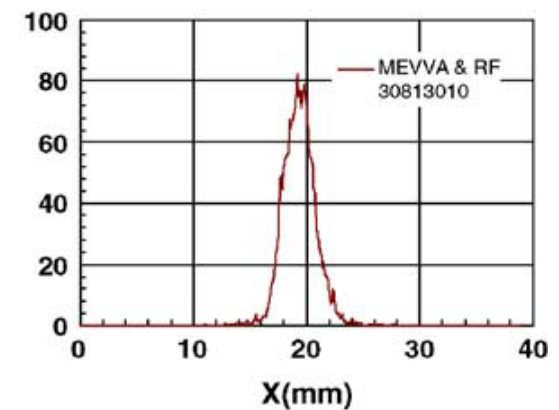
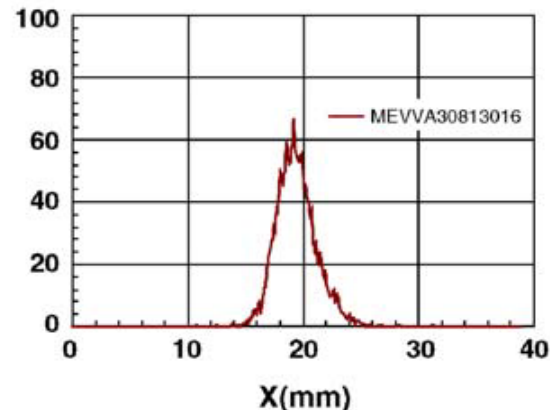
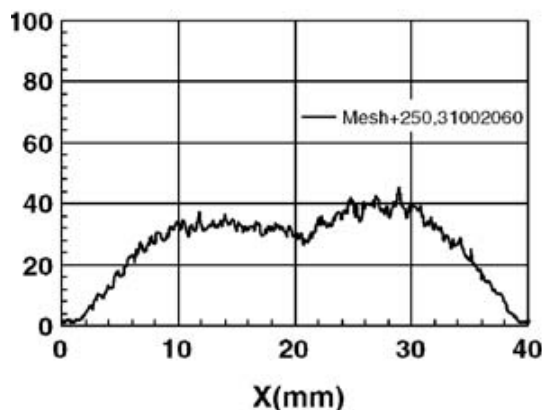


FWHM: 2.83 mm



FWHM: 2.14 mm

P.K. Roy
et al,
NIMPR.
A 544,
225
(2005).



To determine degree of neutralization electron fluid and *full* Maxwell equations are solved numerically and analytically.

$$\frac{\partial \vec{p}_e}{\partial t} + (\vec{V}_e \cdot \nabla) \vec{p}_e = -\frac{e}{m} \left(\vec{E} + \frac{1}{c} \vec{V}_e \times \vec{B} \right), \quad \frac{\partial n_e}{\partial t} + \nabla \cdot (n_e \vec{V}_e) = 0,$$

$$\nabla \times \vec{B} = \frac{4\pi e}{c} (Z_b n_b V_{bz} - n_e V_{ez}) + \frac{1}{c} \frac{\partial \vec{E}}{\partial t}, \quad \nabla \times \vec{E} = -\frac{1}{c} \frac{\partial \vec{B}}{\partial t}.$$

Solved analytically for a beam pulse with arbitrary value of n_b/n_p , in 2D, using approximations: fluid approach, conservation of generalized vorticity.

I. Kaganovich, *et al.*, Phys. Plasmas **8**, 4180 (2001); Phys. Plasmas **15**, 103108 (2008); Nucl. Instr. and Meth. Phys. Res. A **577**, 93 (2007).

Results of Theory for Self-Electric Field of the Beam Pulse Propagating Through Plasma

Self-electric field is determined by electron inertia \sim electron mass

$$eE_r = \frac{1}{c} V_{ez} B_\theta = -mV_{ez} \frac{\partial V_{ez}}{\partial r} \quad \phi_{vp} = mV_{ez}^2 / 2e$$

$$\phi_{vp} = \frac{1}{2} mV_b^2 \left(\frac{n_b}{n_p} \right)^2 = 5eV \left(\frac{n_b}{n_p} \right)^2 \quad V_{ez} \sim V_b n_b / n_p$$

NTX K⁺ 400keV beam $\phi_b \sim 100V$

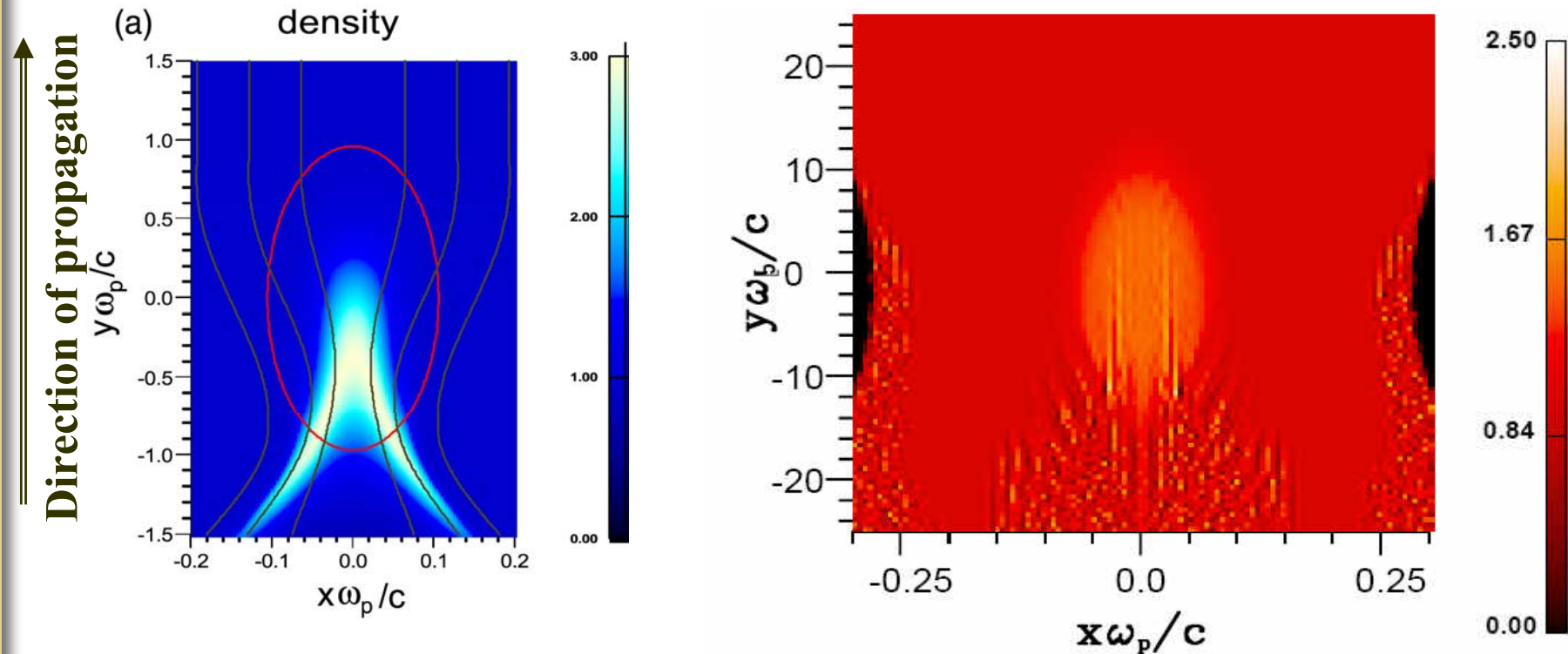
$$(1-f) = \phi_{vp} / \phi_b = 5\% \left(\frac{n_b}{n_p} \right)^2 \quad \text{Degree of neutralization}$$

Having $n_b \ll n_p$ strongly increases the neutralization degree.

$$\mathbf{F}_r = e(\mathbf{E}_r - \mathbf{V}_b \mathbf{B}_\phi / c) \quad F_r = -mV_b^2 \frac{1}{n_p} \left| \frac{\partial n_b}{\partial r} \right|$$

Magnetic force dominates the electrical force and it is focusing!

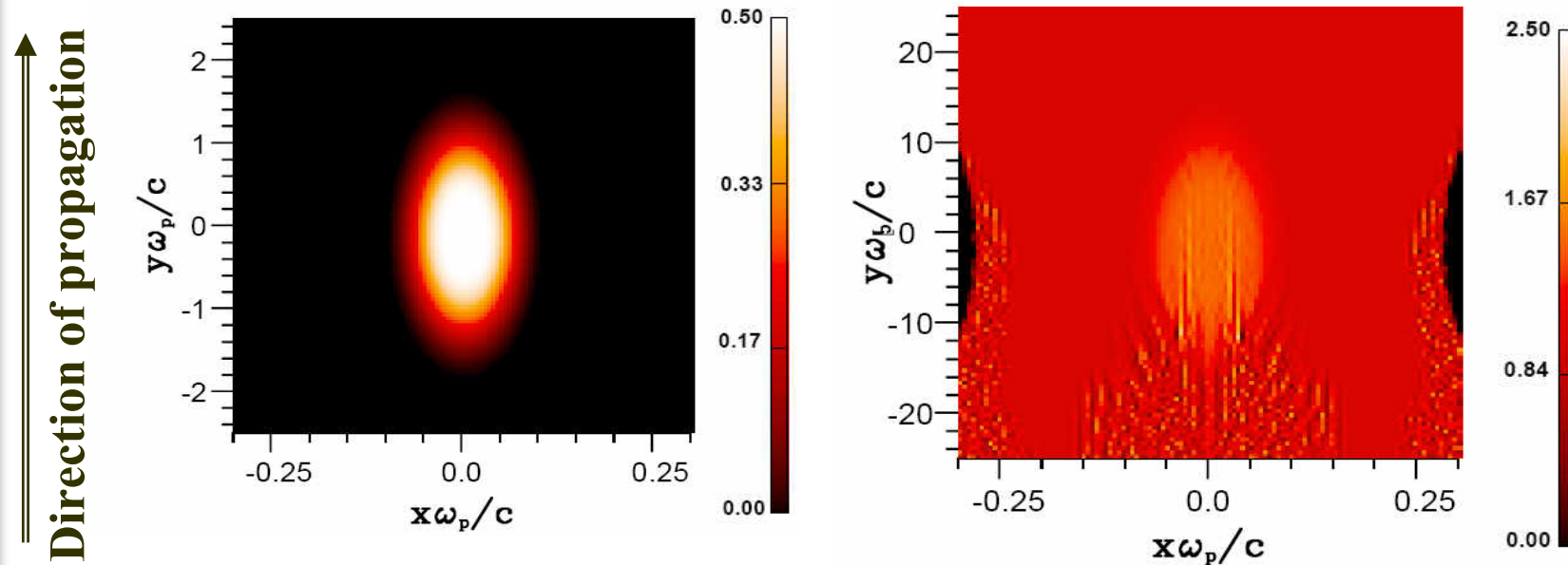
Analytic theory of chamber transport: neutralization and excitation of plasma waves by beam depends on bunch duration and plasma frequency, $\omega_p \tau_b$.



$\omega_p \tau_b$: **a) 4**, **(b) 60**.

Shown in the figure are color plots of the normalized electron density (n_e/n_p), Red line: ion beam size, brown lines: electron trajectory in beam frame, $\beta_b=0.5$, $l_b/r_b=10$, $n_b/n_p=0.5$.

Beam pulse is well neutralized even if its unneutralized potential $\phi_b \ll mV_b^2$

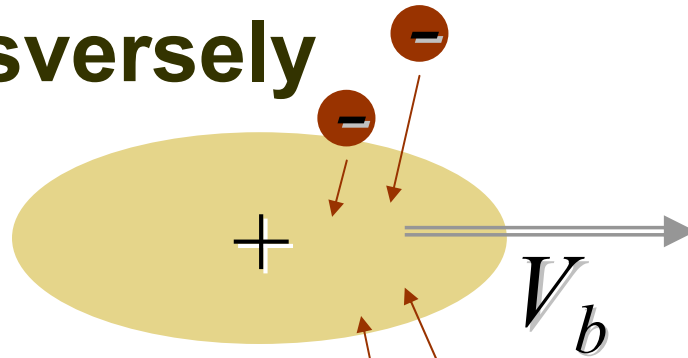


Neutralization of an ion beam pulse. Shown in the figure are color plots of the normalized beam density (n_b/n_p) (left) and the electron density (n_e/n_p), pulse duration $\tau_b\omega_p=60$.

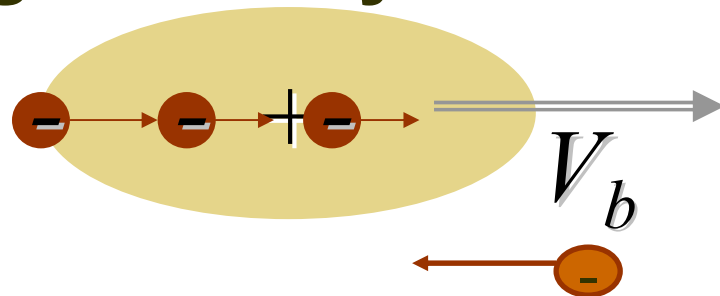
Criterion for neutralization is long pulse duration $\tau_b\omega_p \gg 1$.

Two ways for ion beam pulse to grab electrons to insure full neutralization.

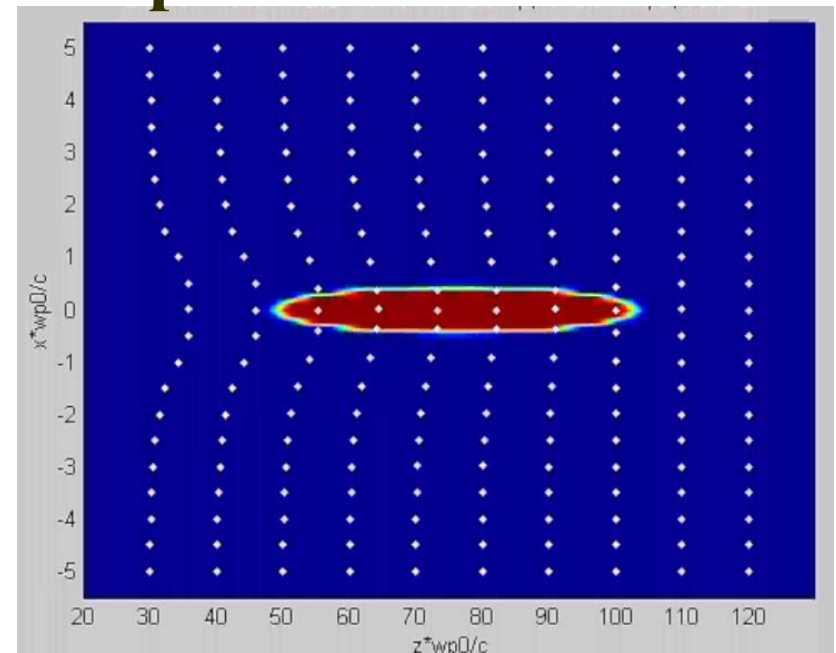
Transversely



Longitudinally

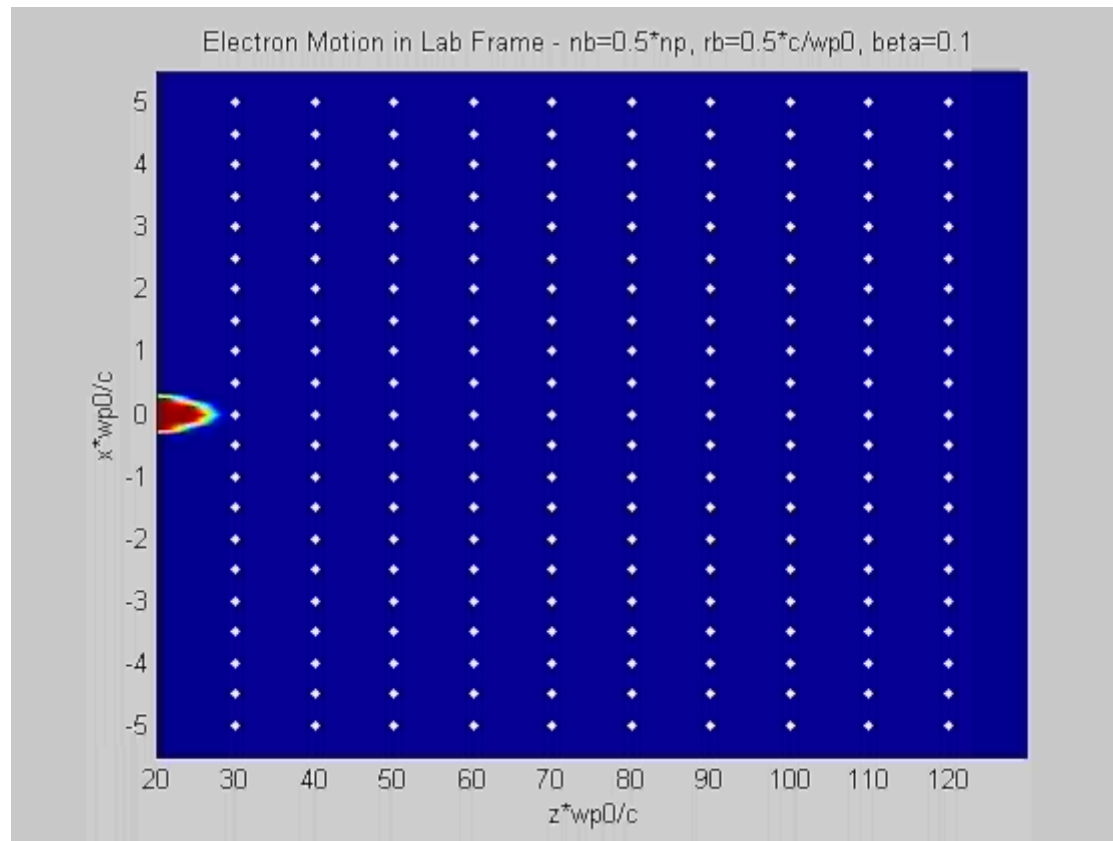


Electron positions in response to ion bunch

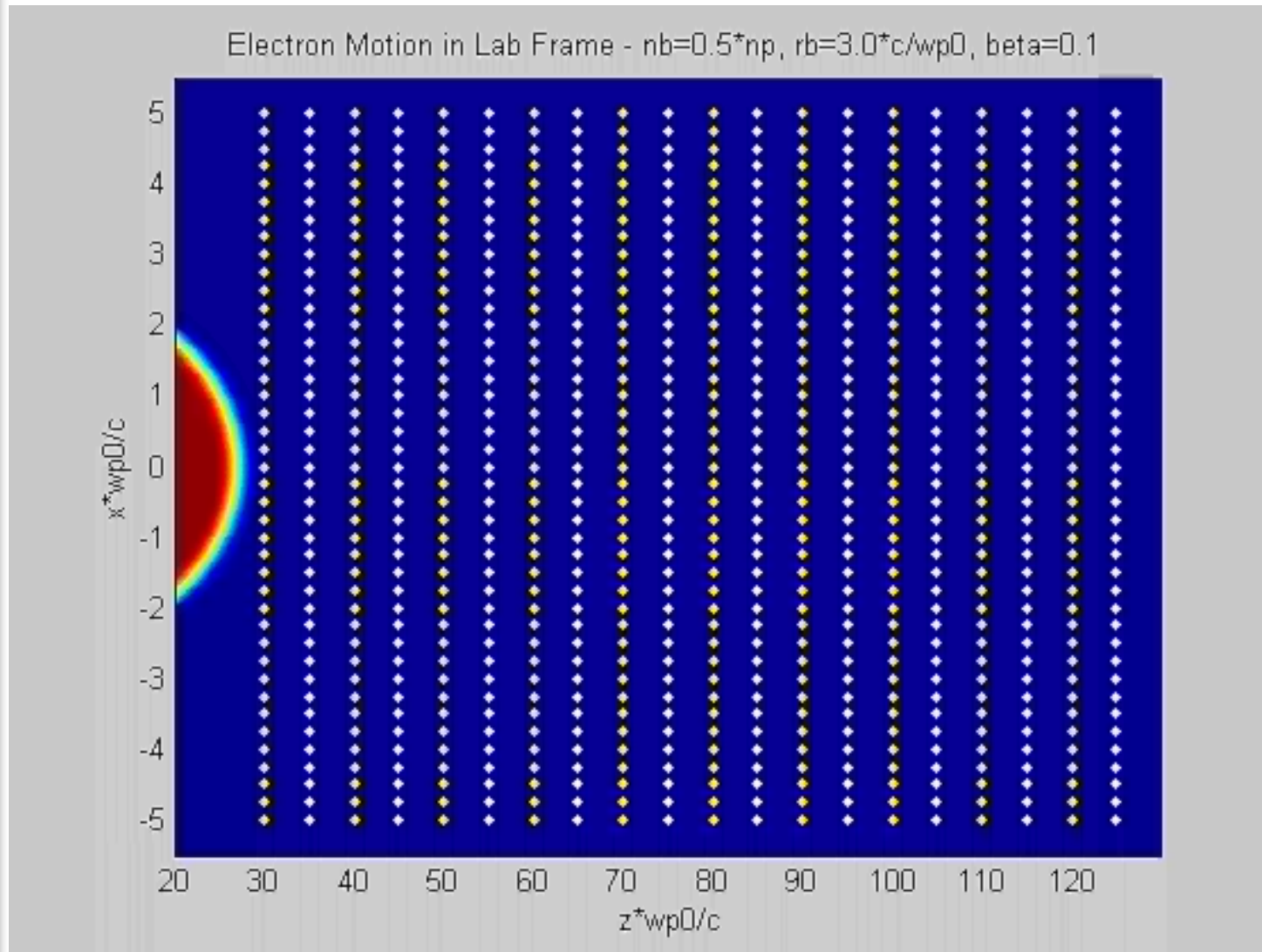


Note in unneutralized beam pulses, electrons accelerate into the beam attracted by space potential: indicating the inductive field is important even for slow beams!

Visualization of Electron Response on an Ion Beam Pulse (thin beam)

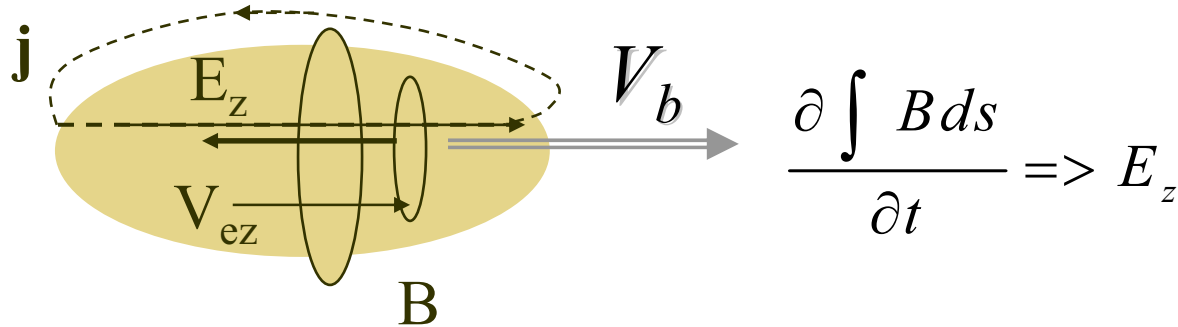


Visualization of Electron Response on an Ion Beam Pulse (thick beam)



Courtesy of B. C. Lyons

Current Neutralization



Alternating magnetic flux generates inductive electric field, which accelerates electrons along the beam propagation*.

For long beams, canonical momentum is conserved** $mV_{ez} = \frac{e}{c} A_z$

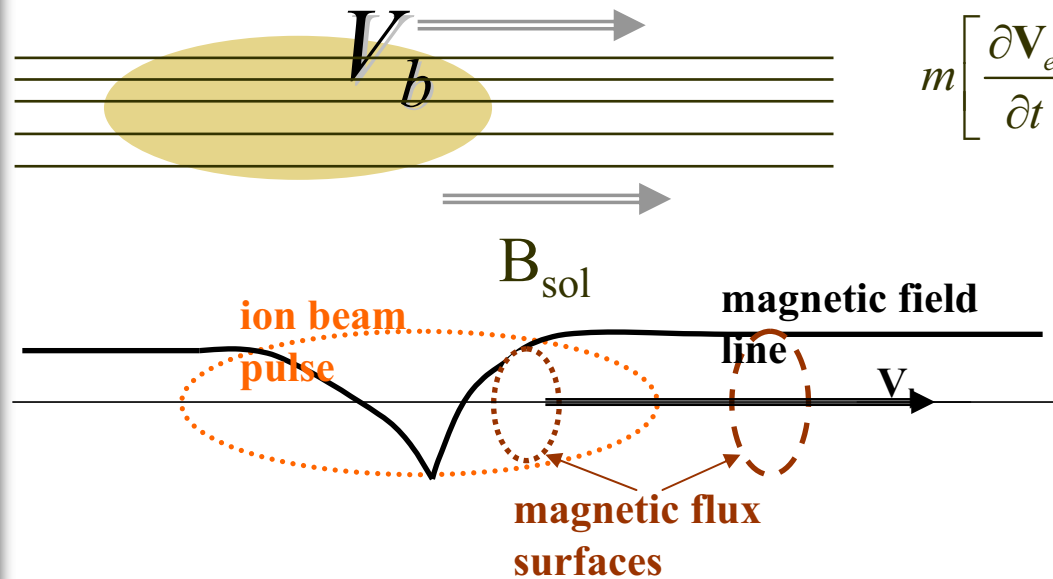
$$\nabla \times \mathbf{B} = \frac{4\pi \mathbf{j}}{c} \quad -\frac{1}{r} \frac{\partial}{\partial r} r \frac{\partial}{\partial r} V_{ez} = \frac{4\pi e}{mc^2} (Z_b n_b V_{bz} - n_e V_{ez}).$$

$$r_b^2 > \frac{c^2}{4\pi e^2 n_p / m} \quad r_b > \delta_p \quad n_p = 2.5 \times 10^{11} \text{ cm}^{-3}; \delta_p = 1 \text{ cm}$$

* K. Hahn, and E. P.J. Lee, Fusion Engineering and Design **32-33**, 417 (1996)

** I. D. Kaganovich, et al, Laser Particle Beams **20**, 497 (2002).

Influence of magnetic field on beam neutralization by a background plasma



$$m \left[\frac{\partial \mathbf{V}_e}{\partial t} + (\mathbf{V}_e \cdot \nabla) \mathbf{V}_e \right] = -e(\mathbf{E} + \frac{1}{c} \mathbf{V}_e \times \mathbf{B})$$

Small radial electron displacement generates fast poloidal rotation according to conservation of azimuthal canonical momentum:

$$V_\phi = \frac{e}{mc} (A_\phi + B_{sol} \delta r)$$

$$E_r \sim \frac{1}{c} V_{e\phi} B_{sol}$$

The poloidal rotation twists the magnetic field and generates the poloidal magnetic field and large radial electric field.

$$B_{e\phi} = B_{ez} \frac{V_{e\phi}}{V_{bz}}$$

Equations for Vector Potential in the Slice Approximation.

$$-\frac{1}{r} \frac{\partial}{\partial r} r \frac{\partial}{\partial r} A_z = \frac{4\pi}{c} j_{bz} - \frac{\omega_{pe}^2}{c^2} A_z - \frac{\omega_{ce}}{V_b} \frac{1}{r} \frac{\partial}{\partial r} (r A_\phi).$$

$$-\left(1 + \frac{\omega_{ce}^2}{\omega_{pe}^2}\right) \frac{\partial}{\partial r} \left[\frac{1}{r} \frac{\partial}{\partial r} (r A_\phi) \right] = \frac{4\pi}{c} j_{b\phi} - \frac{\omega_{pe}^2}{c^2} A_\phi - \frac{\omega_{ce}}{V_b} \frac{\partial}{\partial r} A_z.$$

New term
accounting for
departure from
quasi-neutrality.

Magnetic dynamo

Electron rotation
due to radial displacement

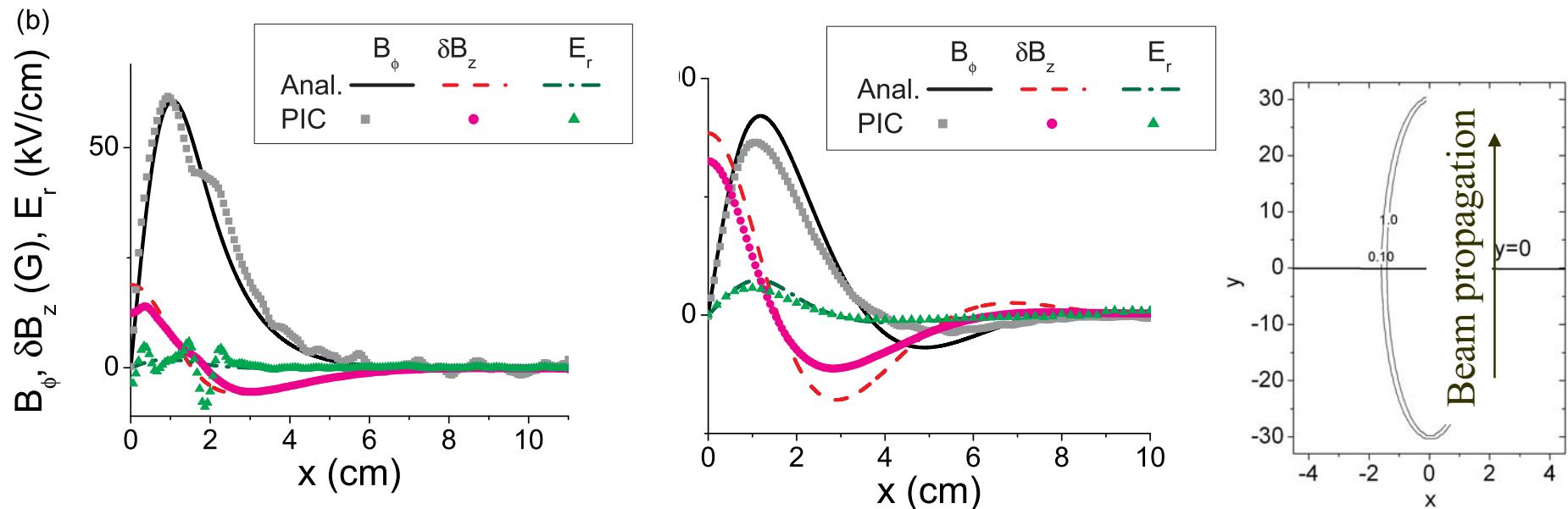
The electron return current

$$\omega_{ce} = \frac{eB_z}{mc}$$

I. Kaganovich, et al, PRL **99**, 235002 (2007); PoP (2008).

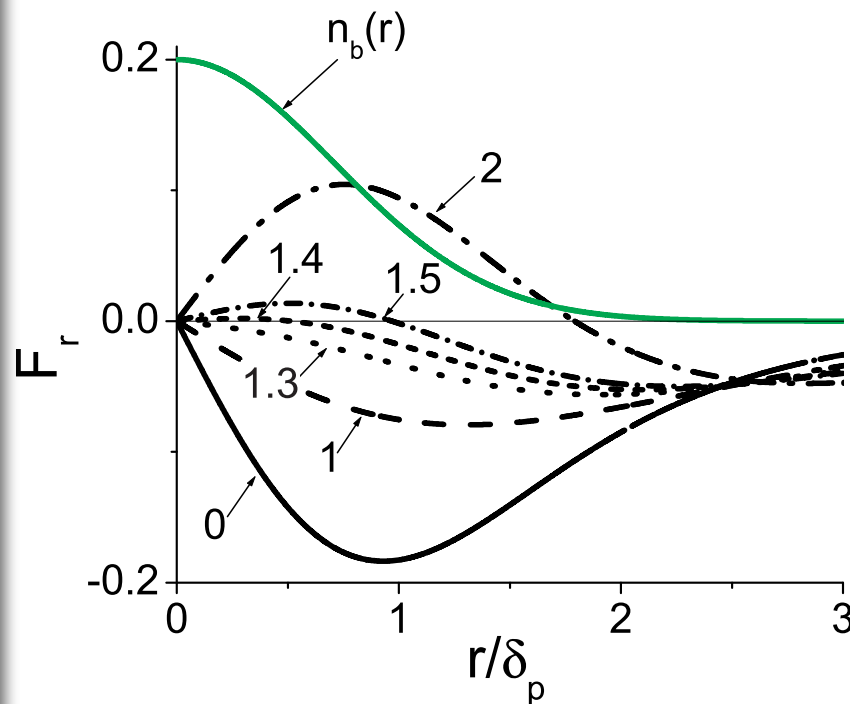
Applied magnetic field affects self-electromagnetic fields when $\omega_{ce}/\omega_{pe} > V_b/c$

Note increase of fields with B_{z0}

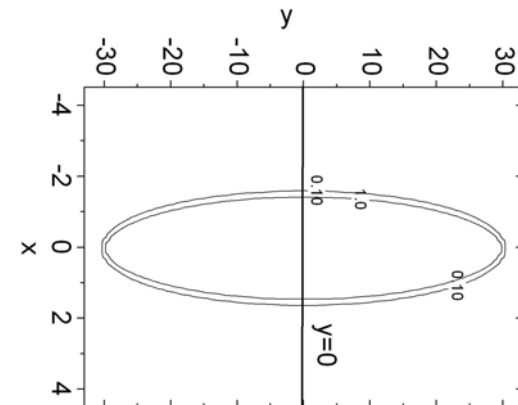


The self-magnetic field; perturbation in the solenoidal magnetic field; and the radial electric field in a perpendicular slice of the beam pulse. The beam parameters are (a) $n_{b0} = n_p/2 = 1.2 \times 10^{11} \text{ cm}^{-3}$; $V_b = 0.33c$, the beam density profile is gaussian. The values of the applied solenoidal magnetic field, B_{z0} are: (b) 300G; and (e) 900G corresponds to $c\omega_{ce}/V_b \omega_{pe} =$ (b) 0.57 ; and (e) 1.7.

Application of the solenoidal magnetic field allows control of the radial force acting on the beam particles.



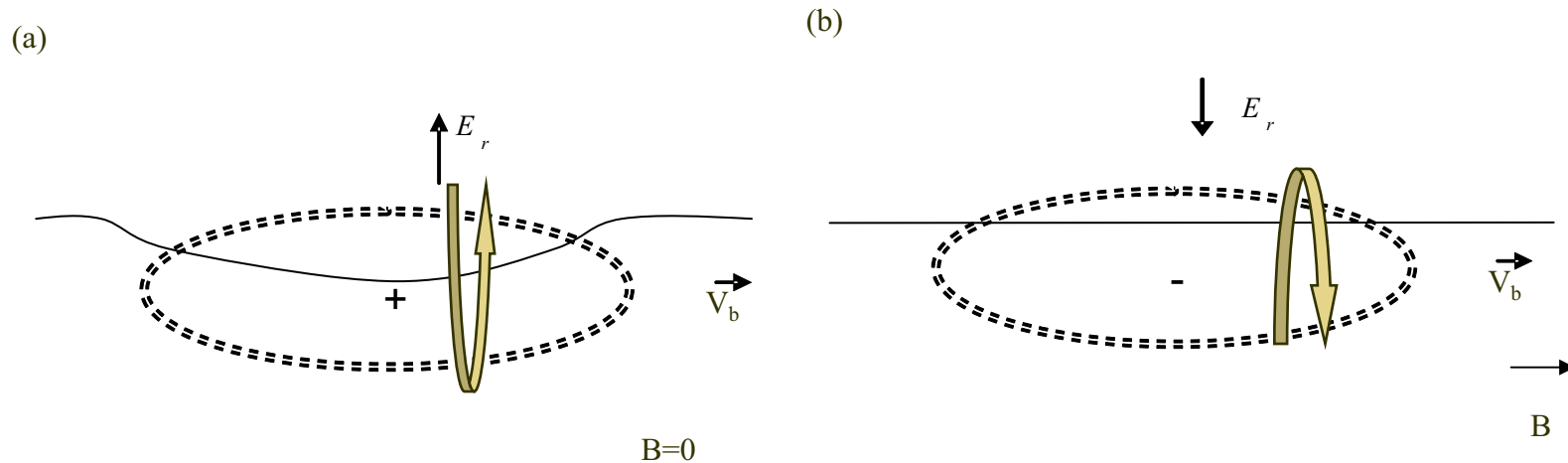
$$\mathbf{F}_r = e(\mathbf{E}_r - V_b \mathbf{B}_\phi / c),$$



Normalized radial force acting on beam ions in plasma for different values of $(\omega_{ce}/\omega_{pe}\beta_b)^2$. The green line shows a gaussian density profile. $r_b = 1.5\delta_p$; $\delta_p = c/\omega_{pe}$.

I. Kaganovich, et al, PRL **99**, 235002 (2007).

Plasma response to the beam is drastically different depending on $\omega_{ce}/2\beta\omega_{pe} < 1$ or > 1



Schematic of an electron motion for the two possible steady-state solutions. (a) Radial self-electric field is defocusing for ion beam, rotation is paramagnetic; (b) Radial self-electric field is focusing for ion beam; rotation is diamagnetic.

Plasma response to the beam is drastically different depending on $\omega_{ce}/2\beta\omega_{pe} < 1$ or > 1

Gaussian beam:
 $r_b = 2c/\omega_{pe}$,
 $l_b = 5r_b$, $\beta = 0.33$

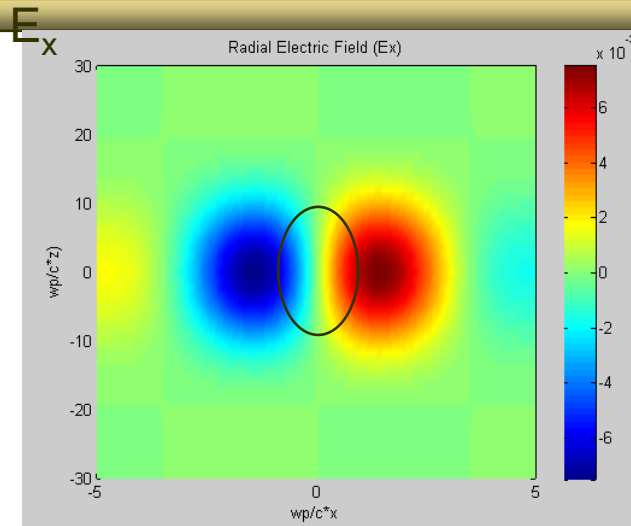
$\omega_{ce}/2\beta\omega_{pe}$

Left: 0.5

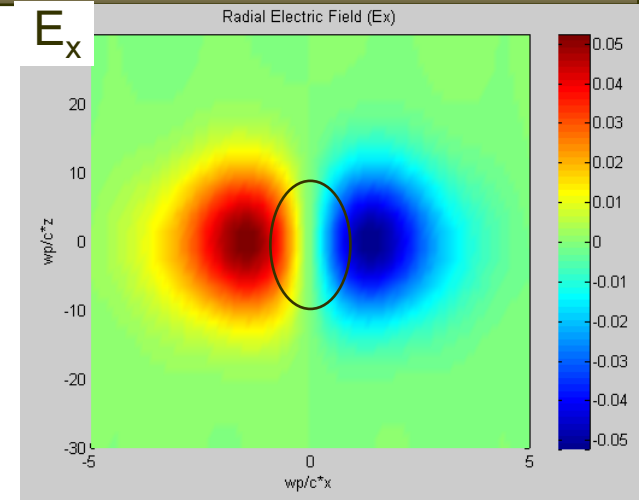
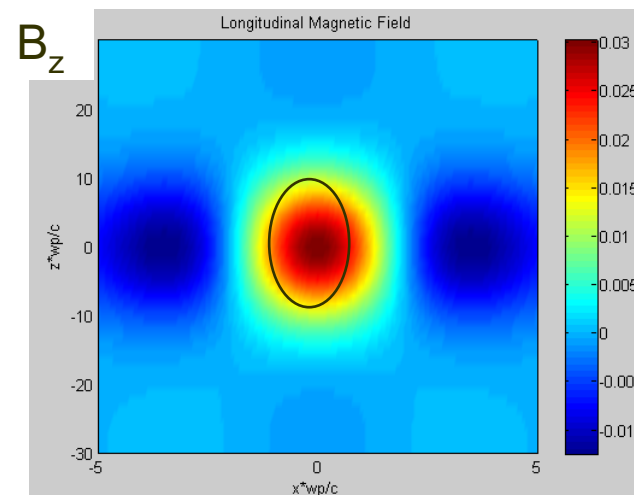
Right: 4.5

M. Dorf, et al, to be submitted PoP (2008).

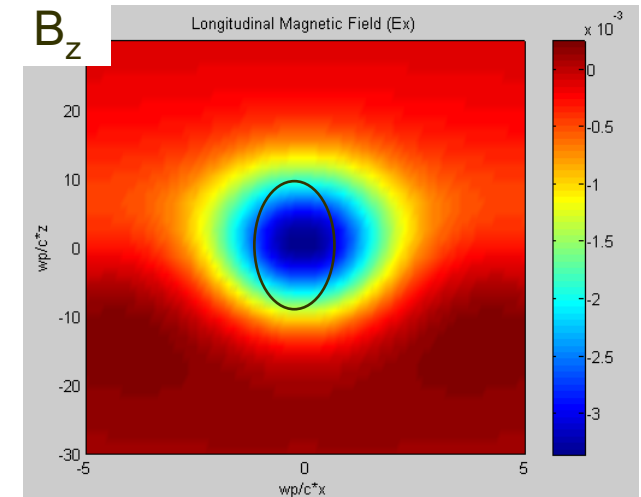
Beam propagation ↑



Electrostatic field is defocusing
 The response is paramagnetic



Electrostatic field is focusing
 The response is diamagnetic



Breaking of the quasi-neutrality condition when $\omega_{ce} > \omega_{pe}$.

$$\mathbf{E}_r \sim m\omega_{ce}^2 r_b / e.$$

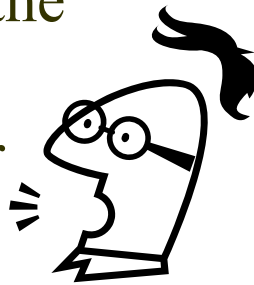
$$dE_r/dr \sim 4\pi en_b,$$

when $\omega_{ce} = \omega_{pe}$.

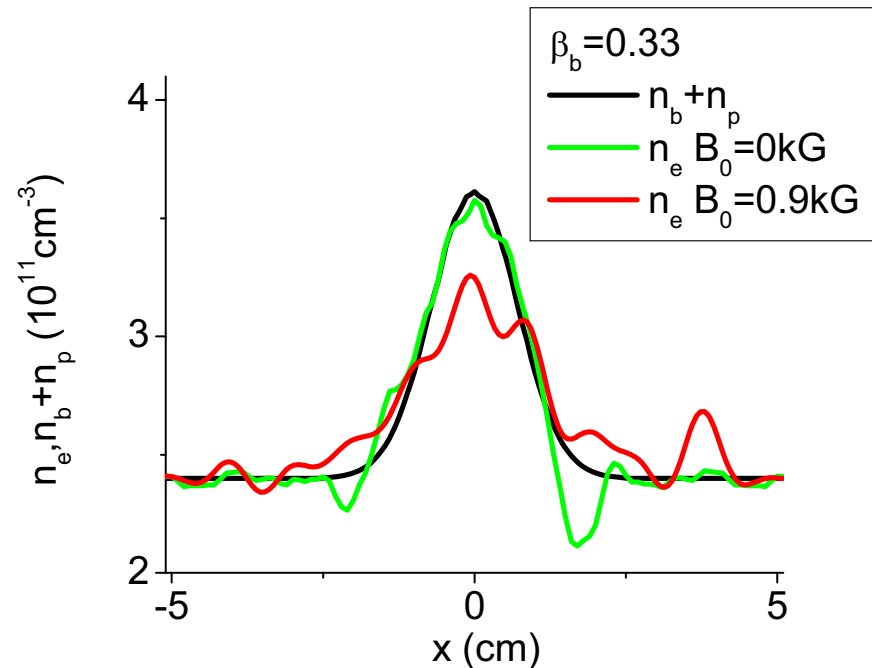
- Consistent with the plasma dielectric constant.

$$\epsilon_{\perp} = 1 - \frac{\omega_{pe}^2}{\omega^2 - \omega_{ce}^2}$$

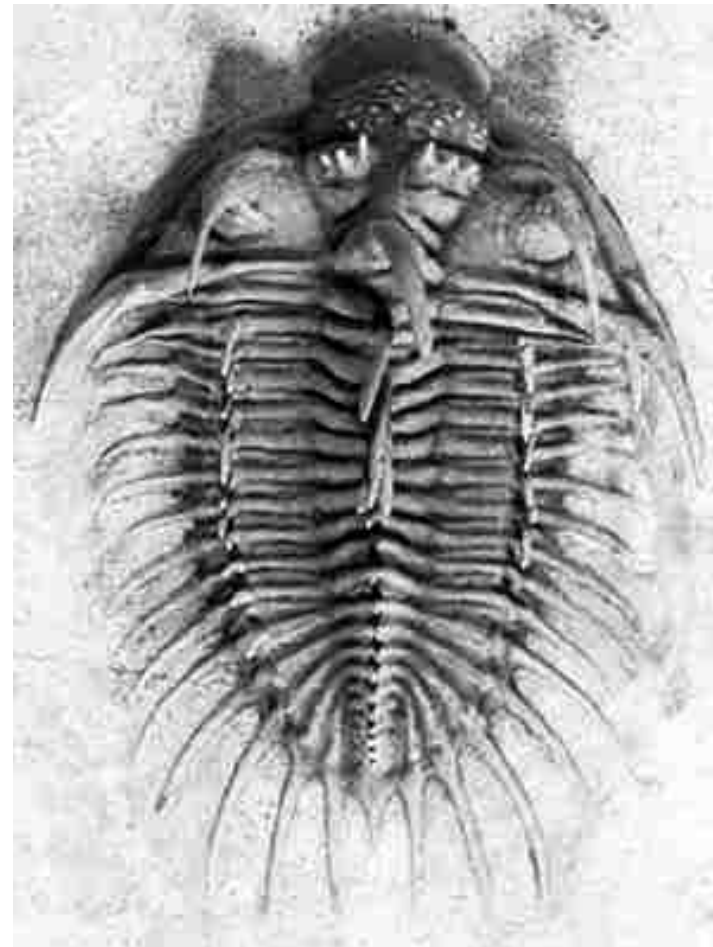
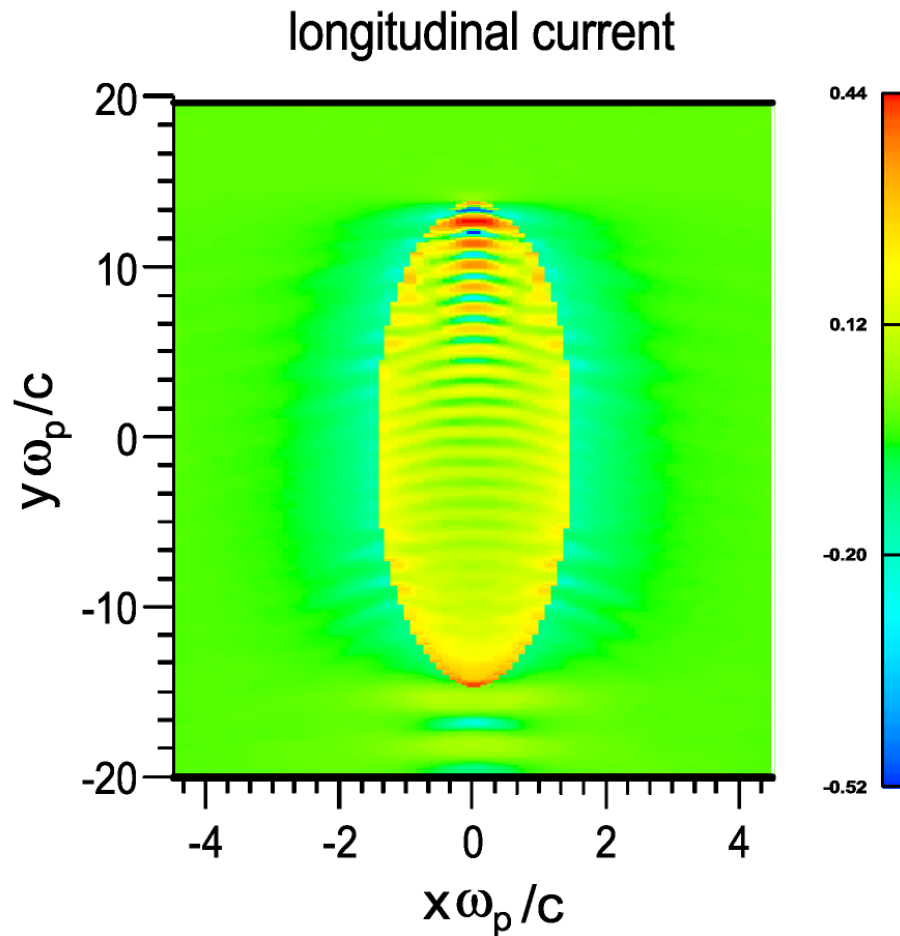
Need to account for the electron density perturbation even for $n_p \gg n_b$!



Radial profile of the electron density perturbation by the beam.
 $\omega_{ce} = 0.5\omega_{pe}$ for $B=0.9\text{kG}$



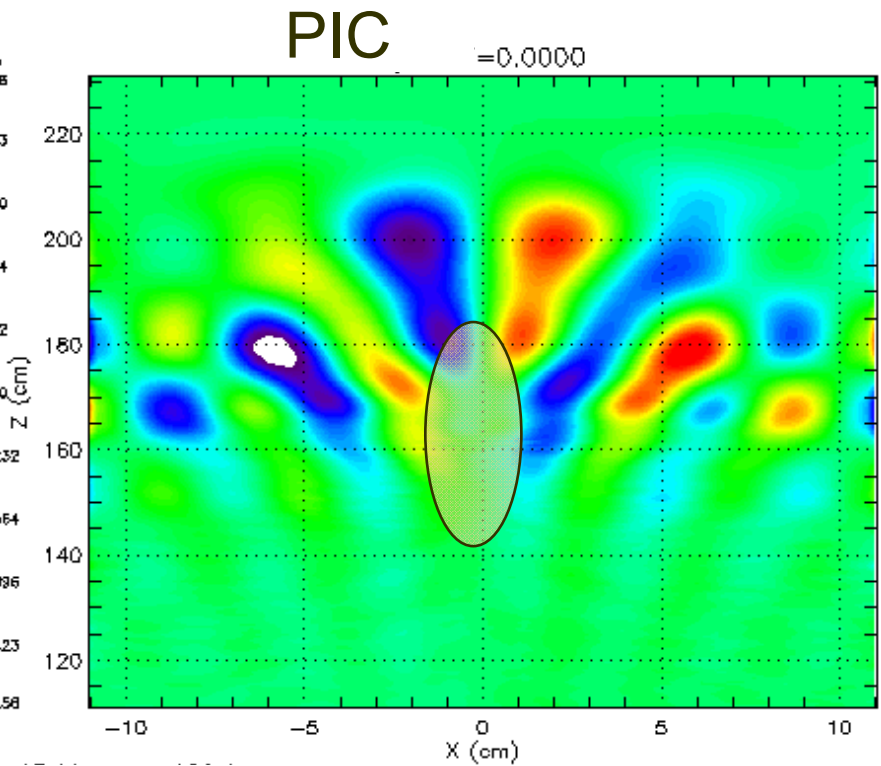
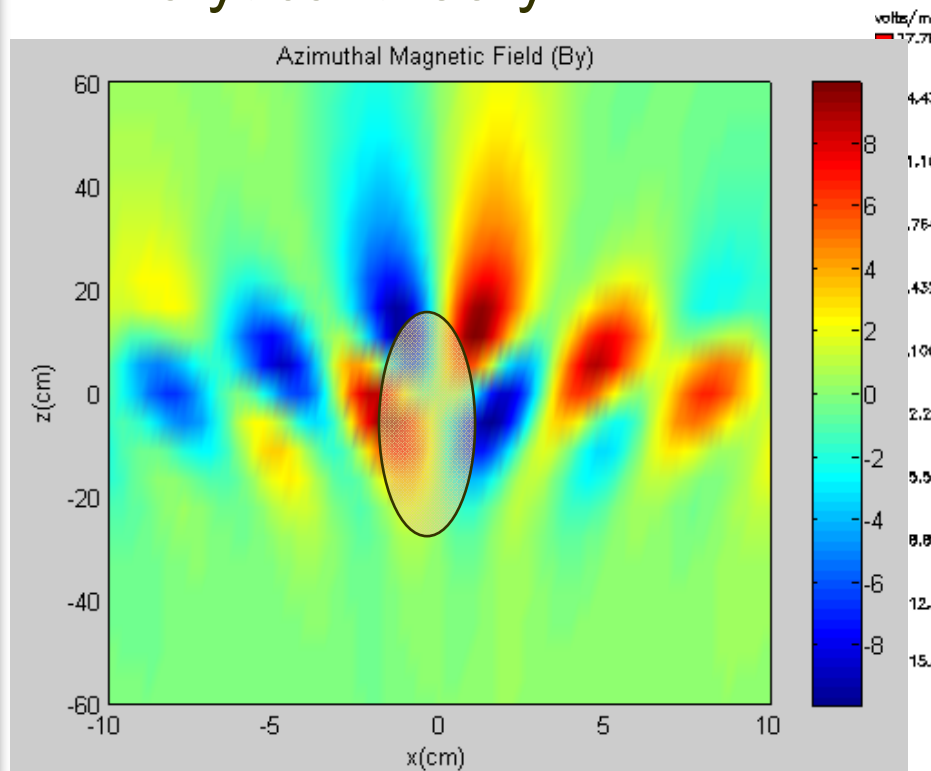
Excitation of plasma waves by the short rise in the beam head.



Beam pulse can excite whistler waves.

Gaussian beam with $\beta=0.33$, $l_b=17r_b$, $r_b=\omega_p/c$ $n_b=0.05n_p$,
 $\omega_{ce}/2\beta_h \omega_{ne}=1.37$

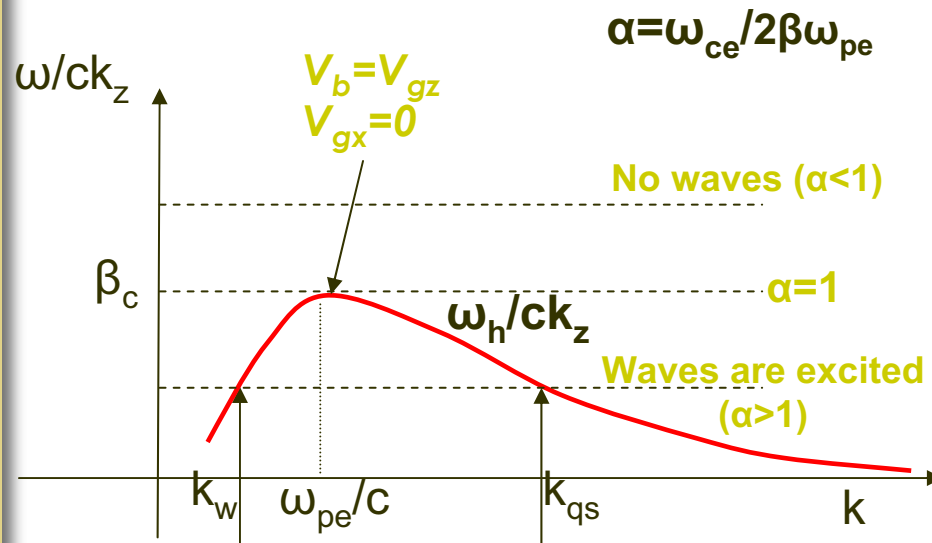
Analytical theory



Courtesy of J. Pennington and M. Dorf

Electromagnetic Field Radiation by a Moving Beam in a Magnetized Plasma

- Beam excites/radiates Helicon (electron) branch $\omega_h = \omega_{ce} k k_z / \left(k^2 + \frac{\omega_{pe}^2}{c^2} \right)$ assumed $\omega_{ce} \ll \omega_{pe}$ for simplicity



Long wavelength Whistler (electromagnetic)

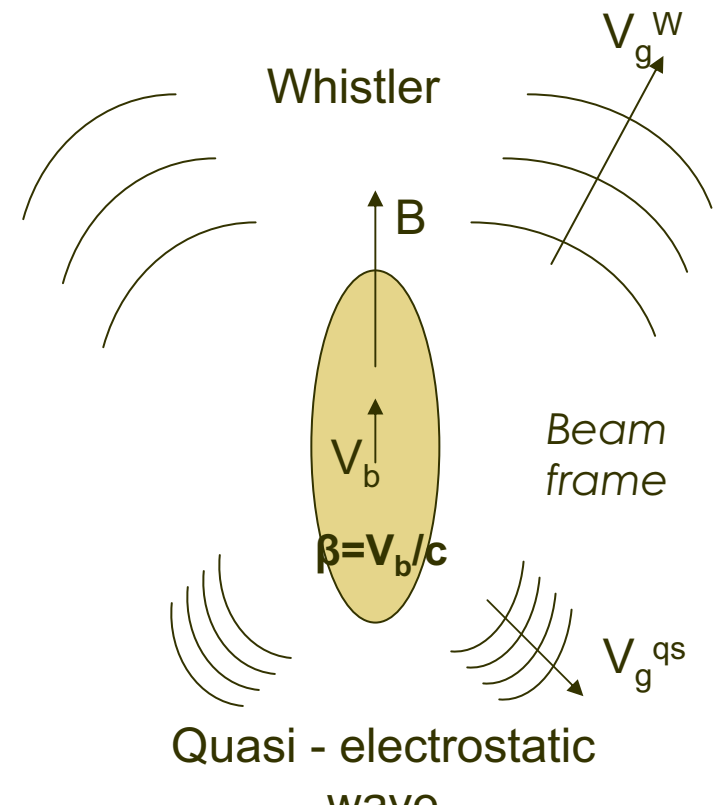
Short wavelength (quasi-electrostatic)

$$V_{gz} > V_b$$

$$V_{gz} < V_b$$

$$k_z V_{gx} > 0$$

$$k_z V_{gx} < 0$$



Courtesy of M. Dorf

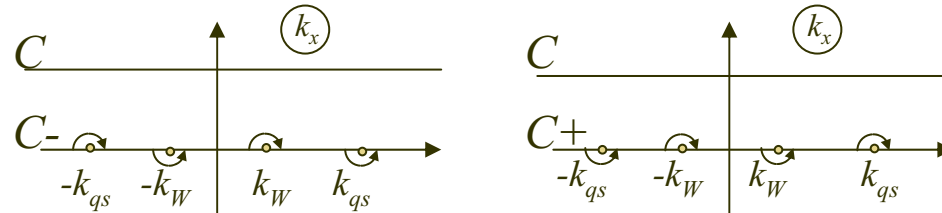
Linear Analytical Theory Method: Laplace Transform and Landau Contours

$$B_y = \frac{\omega_{ce}}{\omega_{pe}} \frac{n_p}{n_{b0}} = \int d\omega \int_{-\infty}^{\infty} \int_{-\infty}^{\infty} dk_z dk_x \frac{n_k}{(\omega - k_z V_b) D(\omega, k_x, k_z)} e^{-i\omega t + ik_x x + ik_z z}$$

Steady state $\omega = k_z V_b$

$$\frac{1}{D(k_z V_b, k_x, k_z)} \cong -i\beta \frac{ck_x / \omega_{pe} (k_x^2 + \omega_{pe}^2 / c^2)}{4\alpha \sqrt{\alpha^2 - 1}} \left[\frac{1}{k_x^2 - k_{qs}^2} - \frac{1}{k_x^2 - k_W^2} \right] \quad \alpha = 2\beta \omega_{pe} / \omega_{ce}$$

Landau contours
(different for $k_z > 0$ and $k_z < 0$)



For a long beam with $n(x, z) = n_z(z) n_x(x)$

$$B_y = \underbrace{n_z(z) \int_C dk_x n_x(k_x) e^{ik_x x} b_k}_C + 2\pi i \int_0^{\infty} dk_z n_z(k_z) \{ \text{res}[-k_{qs}] + \text{res}[k_W] \} + 2\pi i \int_0^{\infty} dk_z n_z(k_z) \{ \text{res}[k_{qs}] + \text{res}[-k_W] \}$$

Local field (decays to zero for $r \gg r_b$)

Can be obtained in the slab approximation

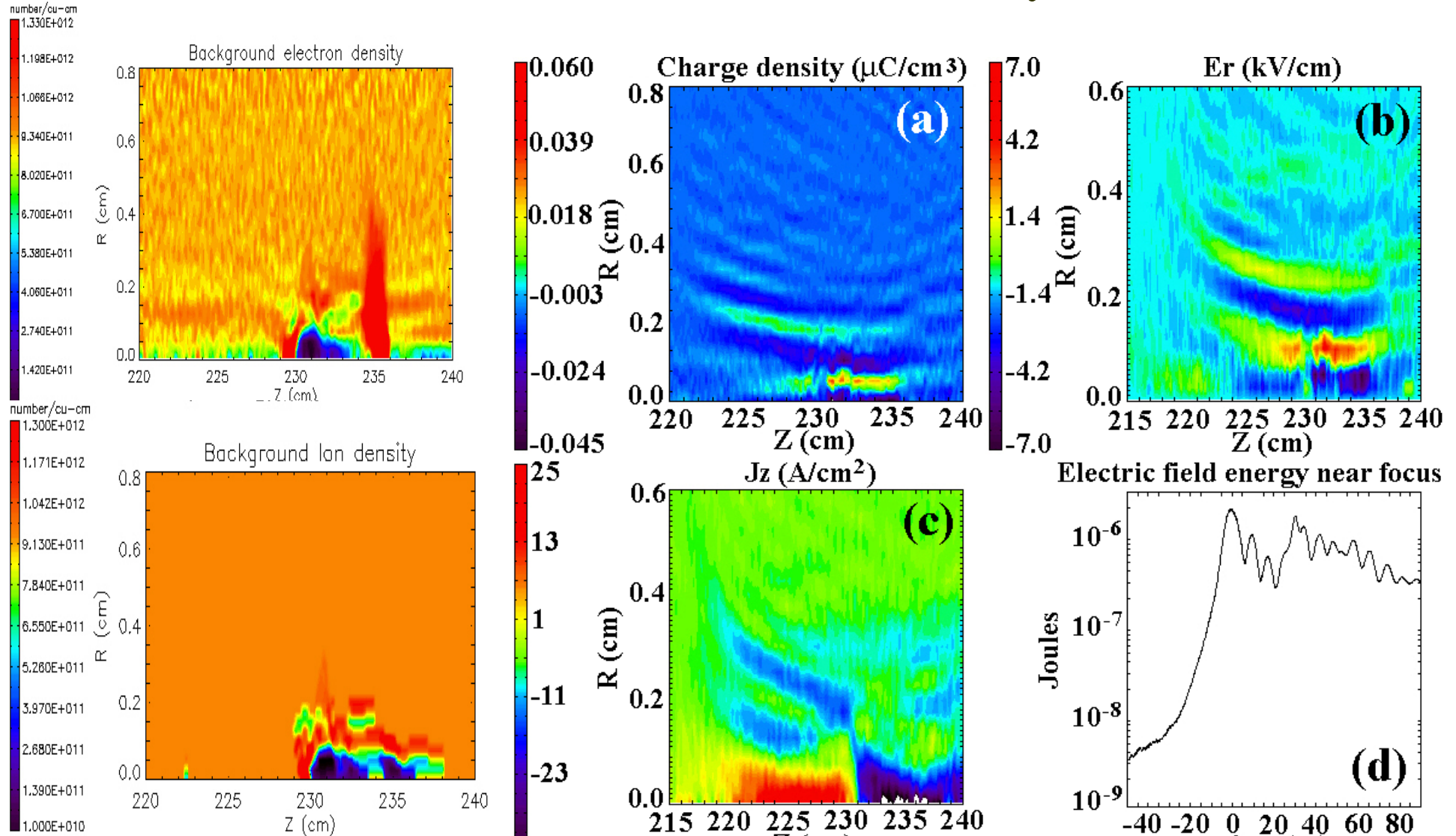
Excited wave field

– slab approximation does not work

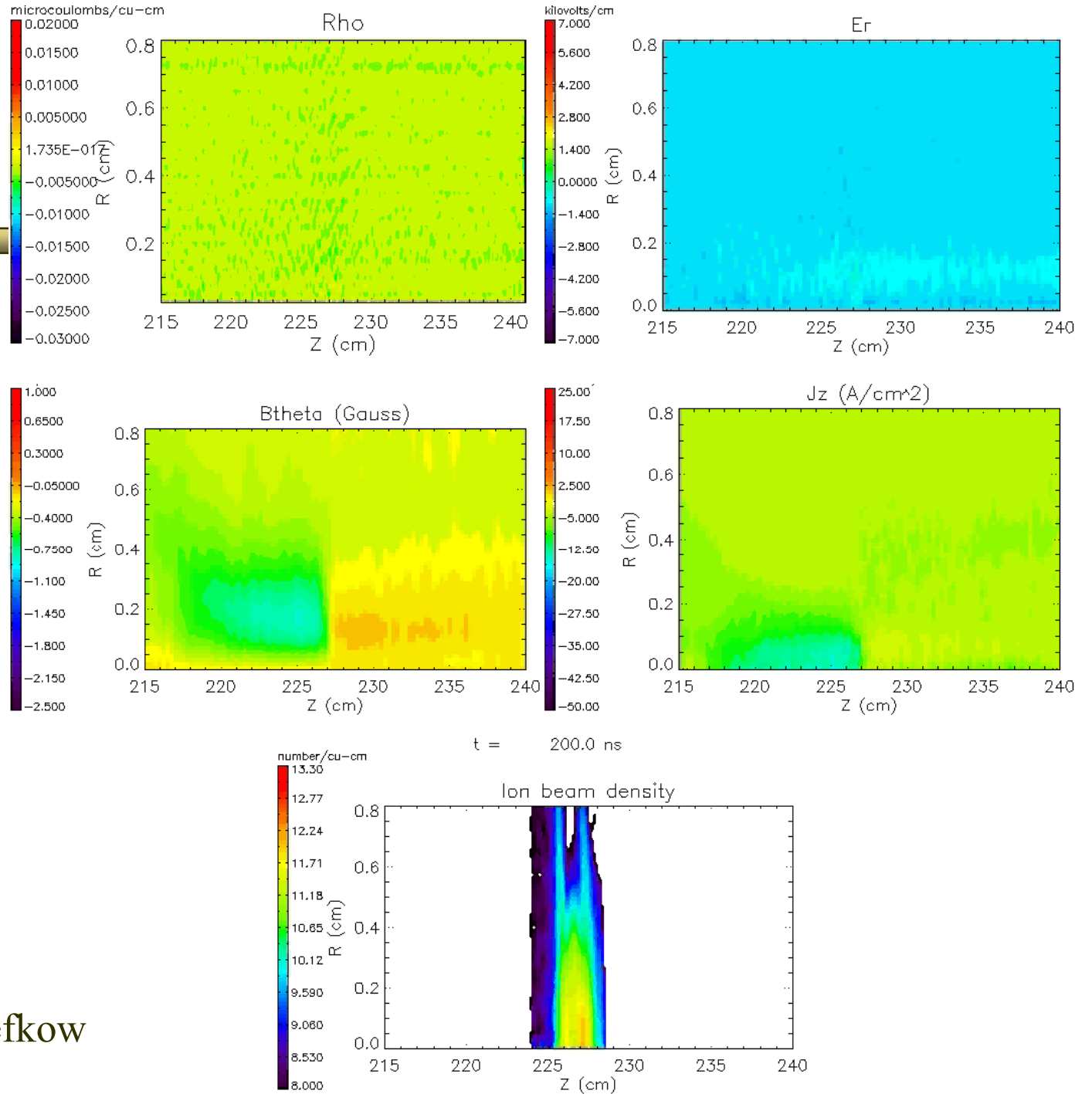
Courtesy of
M. Dorf

During rapid compression at focal plane the beam can excite lower-hybrid waves if the beam density is less than the plasma density.

Courtesy of A. Sefkow

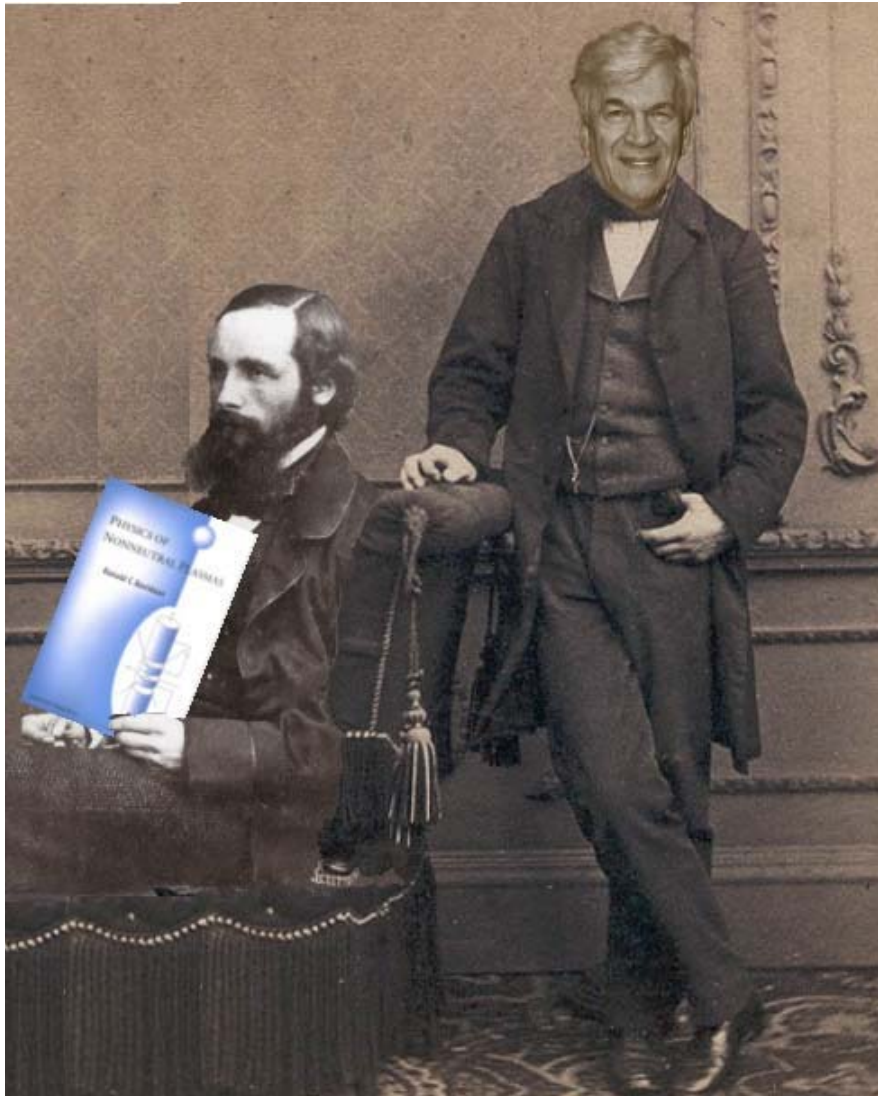


Movies

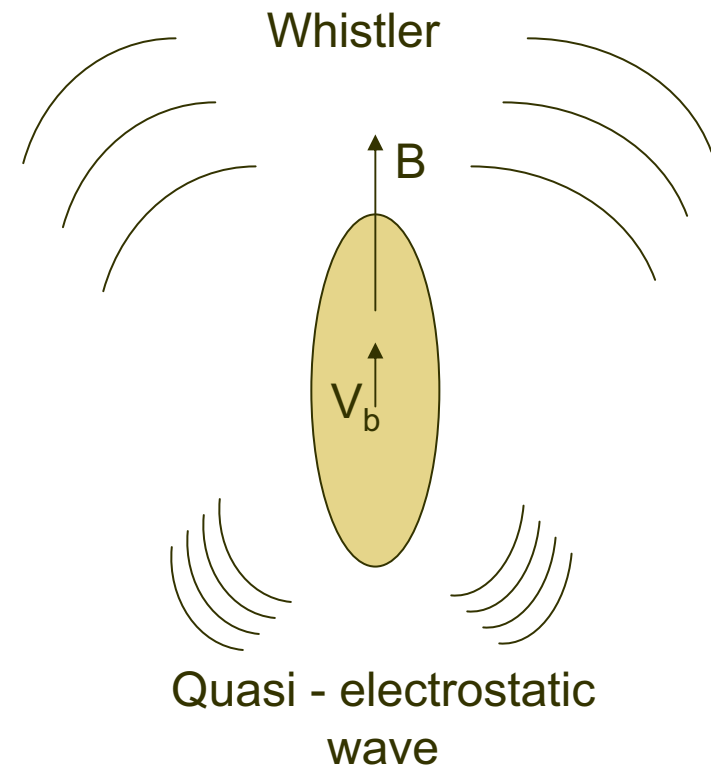


Courtesy of A. Sefkow

Complicated electrodynamics of beam-plasma interaction would make J. Maxwell proud!



**Artist: E.P. Gilson
2008**



Conclusions for neutralization

Developed a nonlinear theory for the quasi-steady-state propagation of an intense ion beam pulse in a background plasma

very good charge neutralization: key parameter $\omega_p l_b / V_b$,

very good current neutralization: key parameter $\omega_p r_b / c$.

Application of a solenoidal magnetic field can be used for active control of beam transport through a background plasma.

Theory predicts that there is a sizable enhancement of the self-electric and self-magnetic fields where $\omega_{ce} \sim \beta \omega_{pe}$.

Electromagnetic waves are generated oblique to the direction of the beam propagation where $\omega_{ce} > \beta \omega_{pe}$.

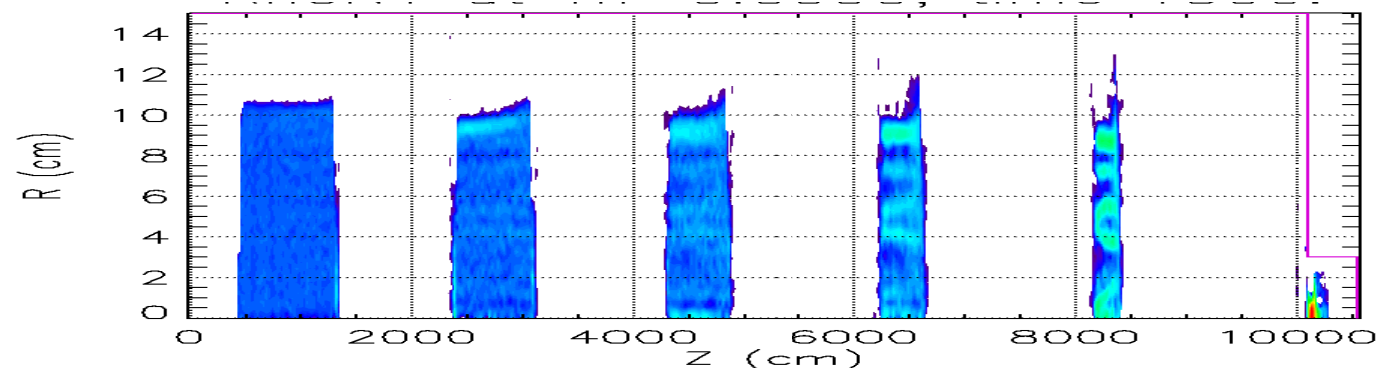
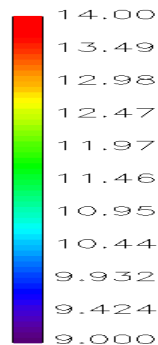
Mitigation of plasma instabilities

- **Two-stream**

- fast, can lead to electron heating.
- mitigated by gradients of the plasma density and beam velocity variation.

- **Weibel (filamentation)**

- slow, can lead to the formation of the beam filaments.
- mitigated by the beam transverse thermal velocity.



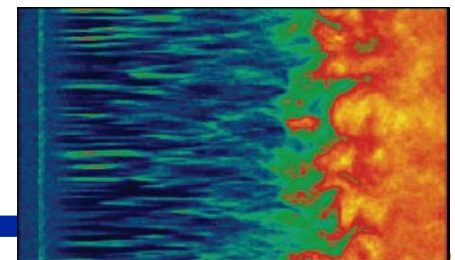
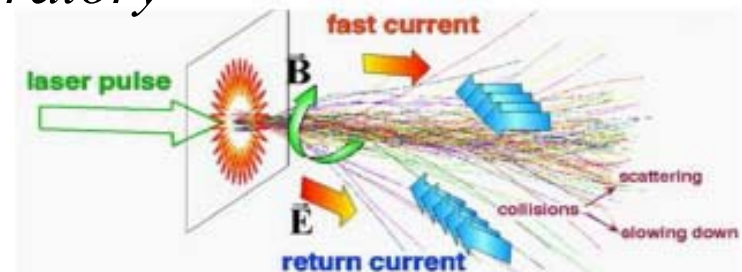
Collisionless ion heating by an intense electron beam due to development of the Weibel instability

Generation of strong magnetic field, beam filamentation, collisionless beam stopping and plasma heating for inertial fusion and astrophysics.

I.D. Kaganovich, E. A. Startsev, A. B. Sefkow
Princeton Plasma Physics Laboratory

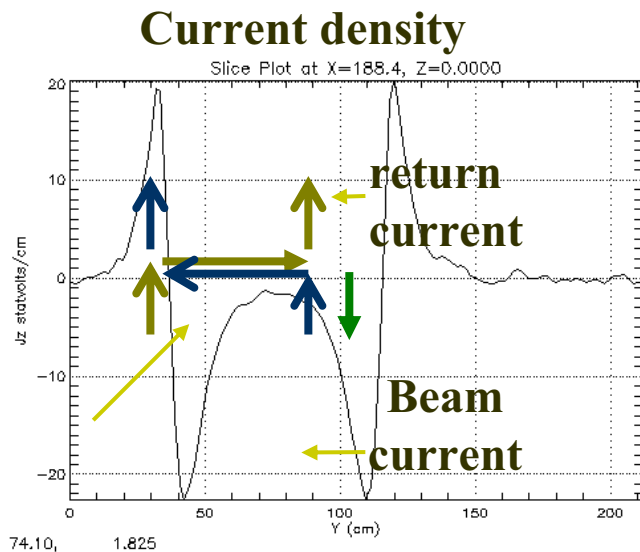
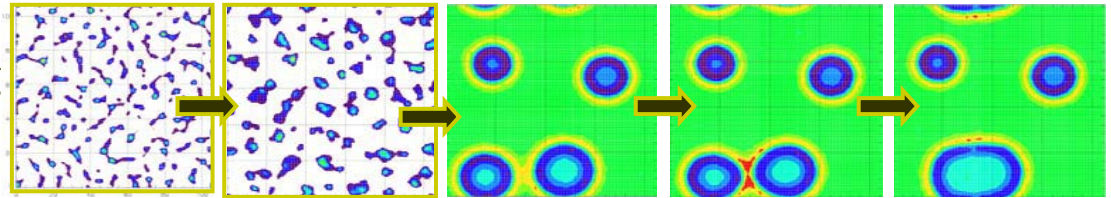
A. Spitkovsky
Princeton University

O. Polomarov and G. Shvets
The University of Texas at Austin

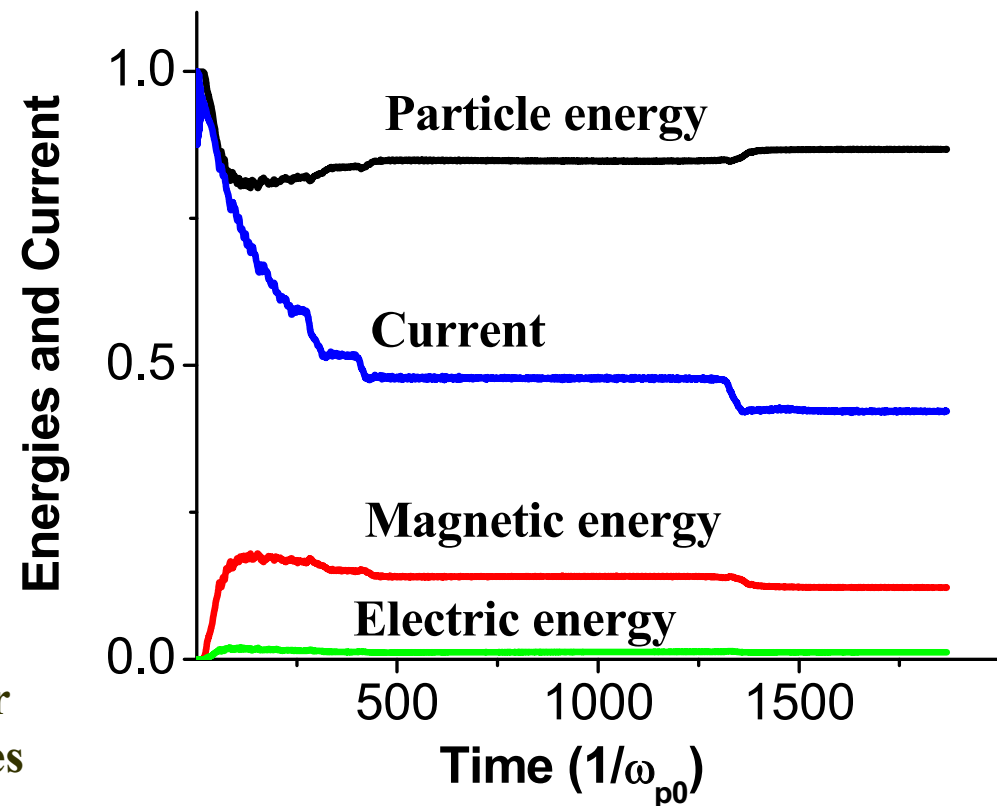


Three Stages of Electron Beam Filamentation

- 1) Linear growth and saturation via magnetic particle trapping
- 2) Nonlinear coalescence of current filaments
- 3) Coalescence of super-Alfvénic current filaments.



Beam current is absent in the center of filament and localized at the edges of the filament.



Movie of the filamentation

$$n_p = 8 \cdot 10^9 \text{cm}^{-3}$$

$$n_b = 2 \cdot 10^9 \text{cm}^{-3}$$

$$\gamma_b = 3.3$$

Analytic solution for filament structure

$\mathbf{B} = -\mathbf{e}_z \times \nabla \psi$ Vector potential, magnetic flux

Conservation of canonical momentum for beam and plasma

electrons: $m\gamma_b v_{bz} - \frac{e}{c}\psi = m\gamma_b v_{bz0}$ $mv_{be} - \frac{e}{c}\psi = 0$

Quasineutrality: $n_i = n_b + n_e$

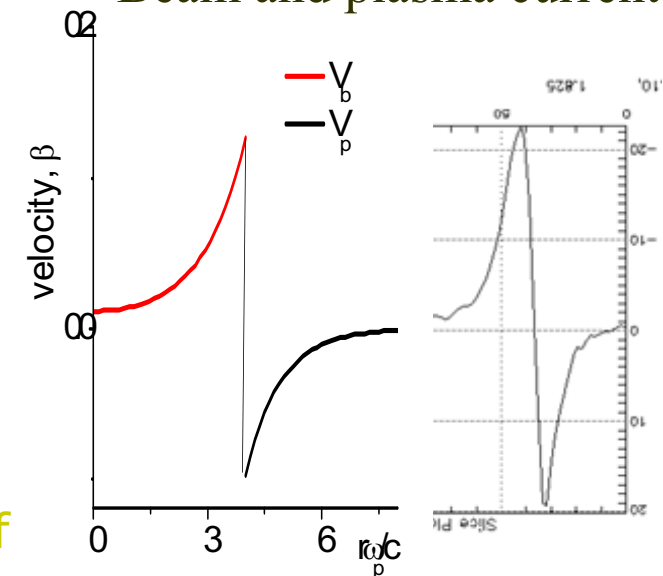
Ampere's law:

$$\nabla^2 \psi - \frac{4\pi e^2}{mc} n_i \psi = 4\pi e n_b \beta_{b0}$$

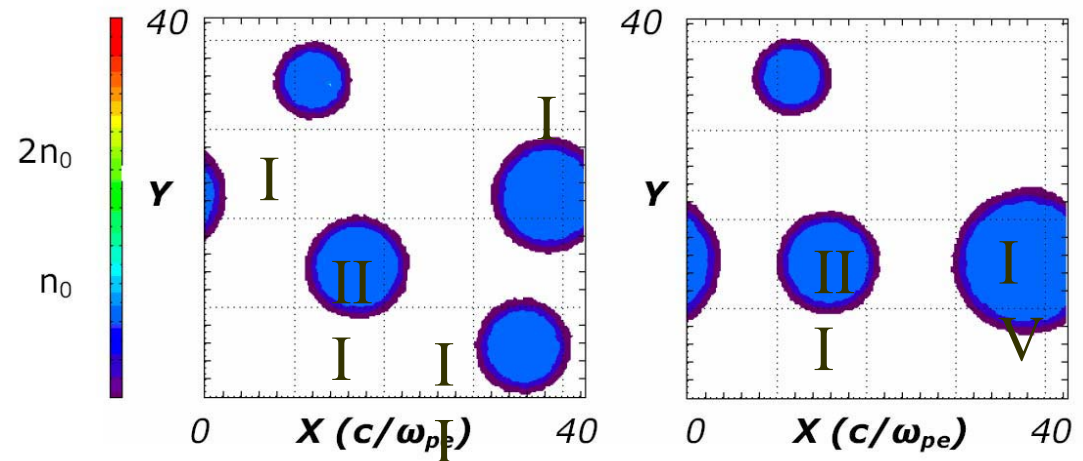
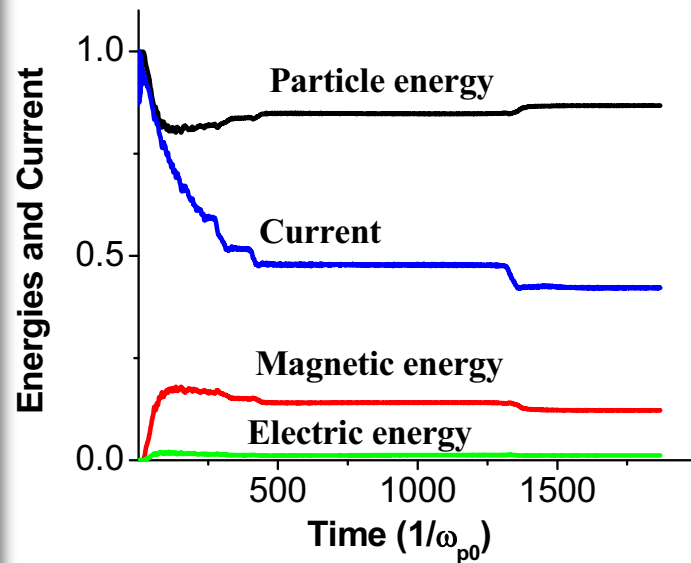
The beam part of the solution has the form of the Hammer-Rostoker beam equilibrium.

Theory versus PIC

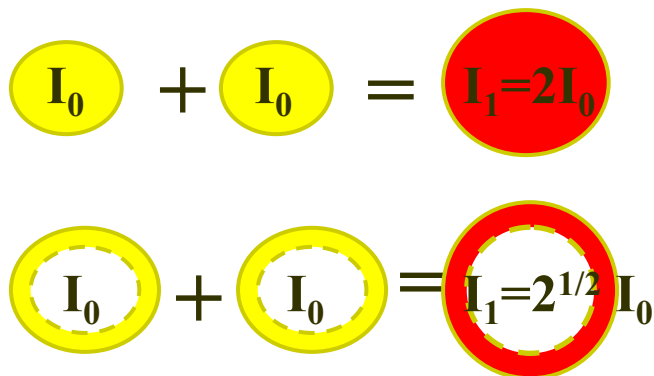
Beam and plasma current



Magnetic energy decrease as a result of merger of large filaments, $I > I_A$



**Current I: $2.4I_A$, Current II: $2.7I_A$,
Resulting current IV: $4.5I_A$**

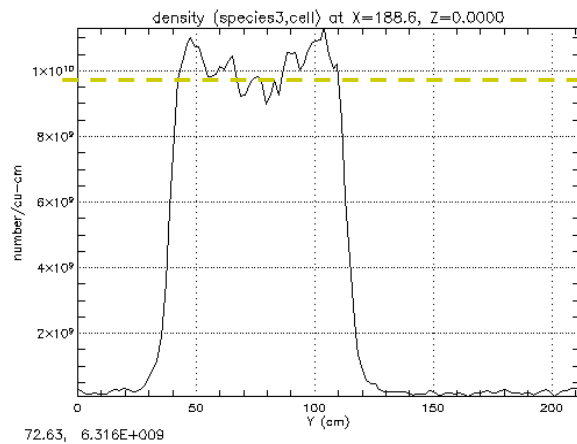


In small filaments, the current flows throughout the entire beam cross section \rightarrow the current doubles \rightarrow the magnetic energy doubles.

In large filaments, the current flows only at the periphery of the beam \rightarrow the magnetic energy decreases.

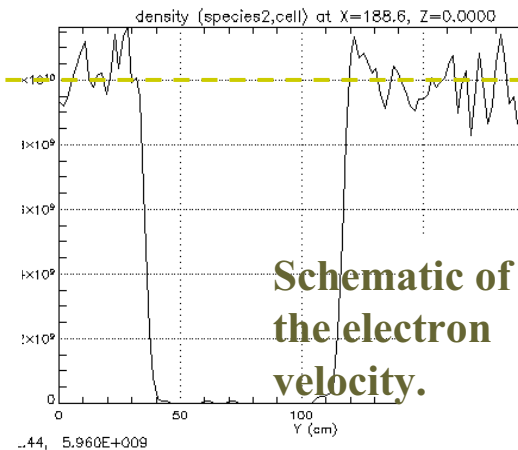
Super-Alfvénic filaments, $I > I_A = \gamma mc^3/e$

Beam density



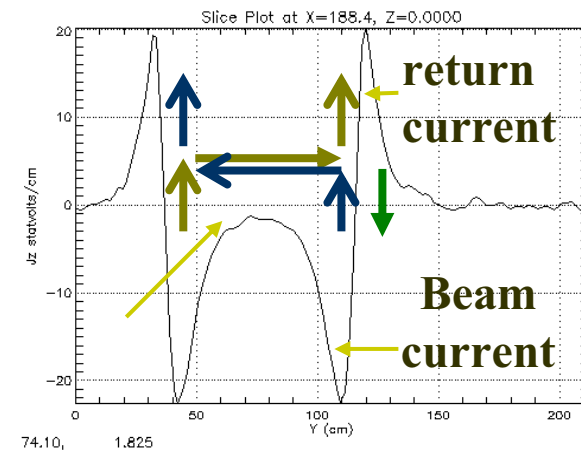
Beam density is equal to the back-ground ion density in the filament and sharply decreases at the periphery of the filament.

Plasma density



Ambient plasma is fully expelled from the filament.

Current density



Beam current is absent in the center of filament and localized at the edges of the filament.

Large radial electric field can cause ion heating

$$n_p = 8 \cdot 10^9 \text{cm}^{-3}$$

$$n_b = 2 \cdot 10^9 \text{cm}^{-3}$$

$$\gamma_b = 3.3$$

Operation of the Hall thruster with intense secondary electron emission

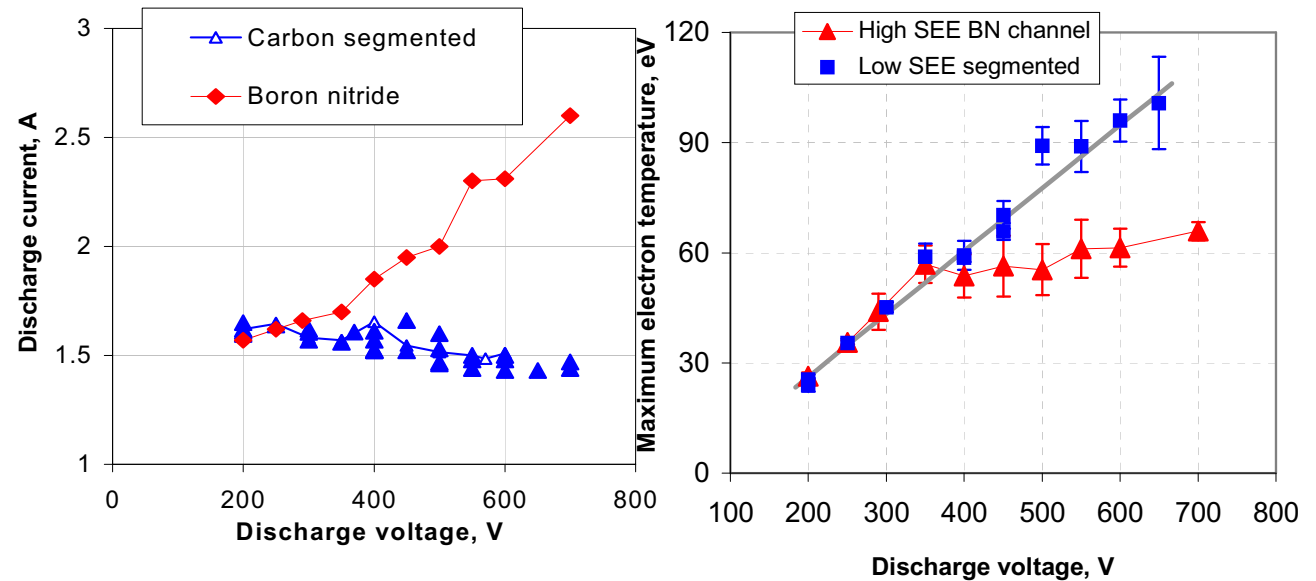
Igor Kaganovich, Yevgeny Raitses*

Dmytro Sydorenko, Andrei Smolyakov**

**Princeton Plasma Physics Laboratory, USA*

***University of Saskatchewan, Canada*

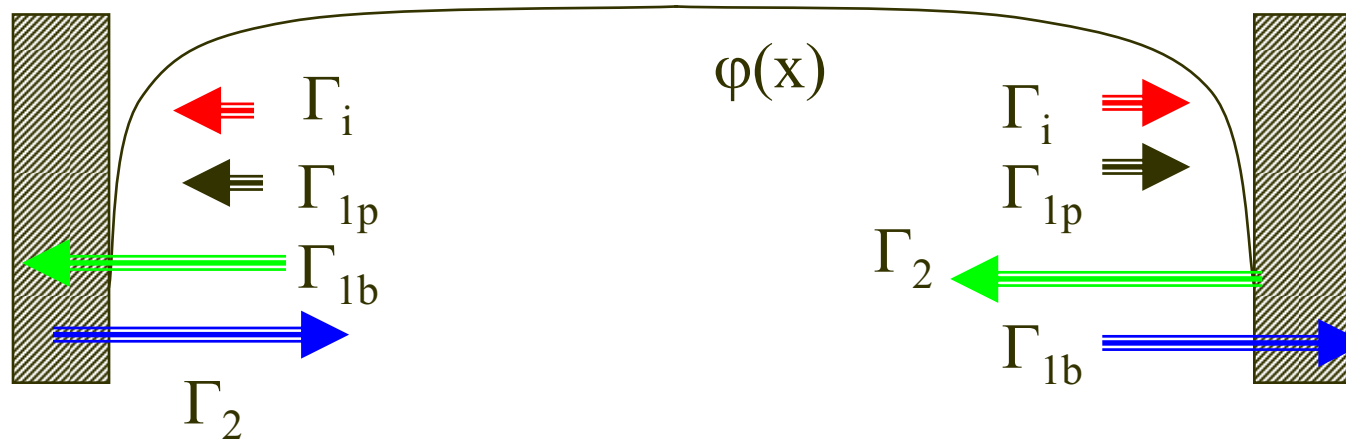
Study of a 2 kW PPPL Hall Thruster with low and high secondary electron emission (SEE) segmented electrodes.



- Channel walls made from boron nitride, which provides **high SEE**.
- Carbon-based segmented electrodes (floating), with **low SEE**.

From: Y. Raitses et. al, J. Appl. Phys. **99**, 036103 (2006);
Phys. Plasmas **13**, 014502 (2006).

The balance of the SEE fluxes from the opposite walls affects the wall potential.



1- primary

2- secondary

SEE coefficients:

$\gamma_p \equiv \Gamma_{2p} / \Gamma_{1p}$ - SEE due to plasma electrons

$\gamma_b \equiv \Gamma_{2b} / \Gamma_{1b}$ - SEE due to beam electrons

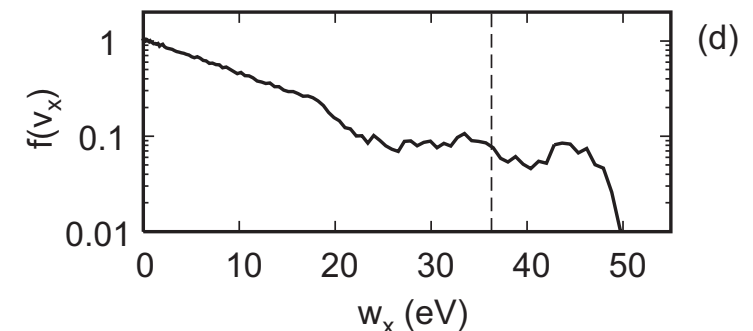
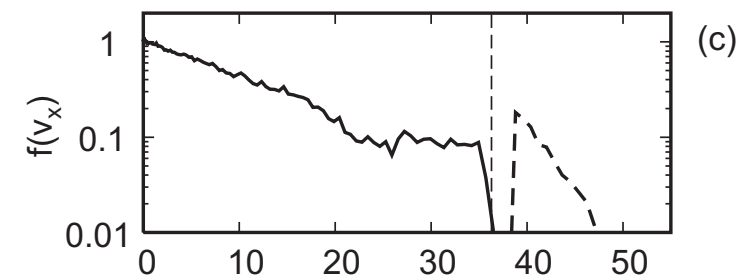
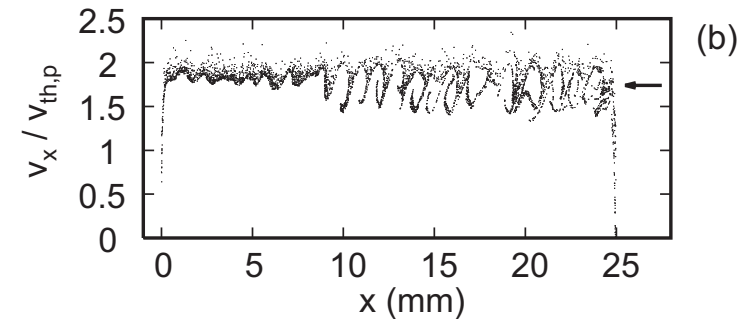
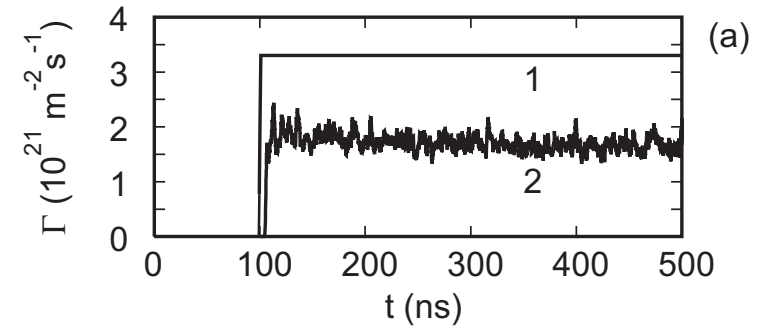
$\alpha \equiv \Gamma_{1b} / \Gamma_2$ - penetration coefficient of the SEE beams

$$\Gamma_i = \Gamma_{1p} \left(1 - \gamma_p \frac{1 - \alpha}{1 - \alpha \gamma_b} \right)$$

The two-stream instability of secondary electron beams

Non-monotonic emission EVDF

- (a) The penetrated electron beam flux (curve 2) is about two times smaller than the emitted one (curve 1).
- (b) Phase plane ($t = 499$ ns) shows the intense permanently existing two-stream instability.
- (c) The total EVDF (solid line – plasma, dashed line - beam) near the emitting wall ($x=0$) remains non-monotonic.
- (d) *The total EVDF near the target wall ($x=25$ mm) has a plateau.*
- **The two-stream instability results in decrease of the SEE fluxes penetrating through the plasma.**
- **The penetration coefficient (the ratio of penetrated and emitted fluxes) is $\alpha < 1$.**

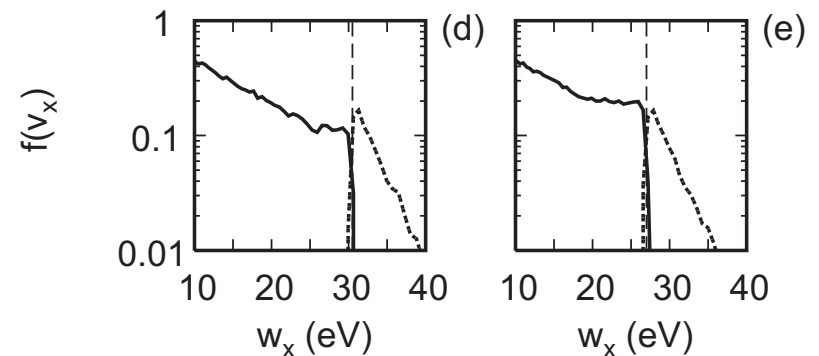
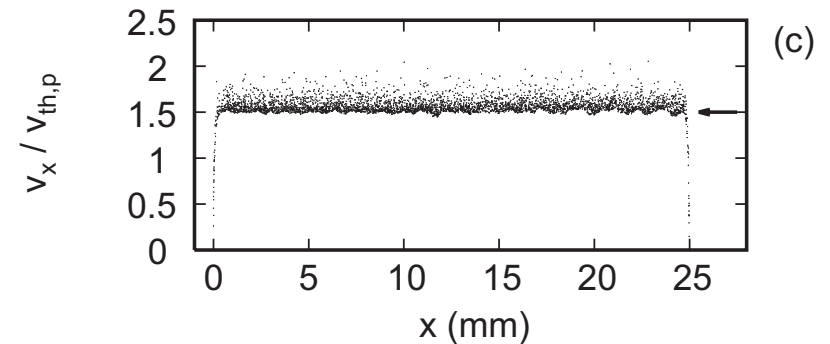
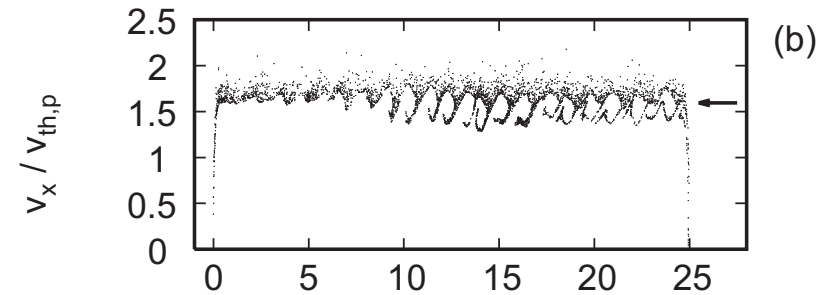
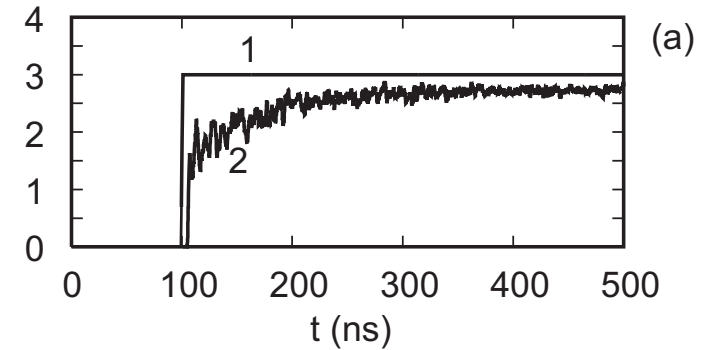


The two-stream instability of secondary electron beams

 $\Gamma (10^{21} \text{ m}^{-2} \text{ s}^{-1})$

Monotonic emission EVDF

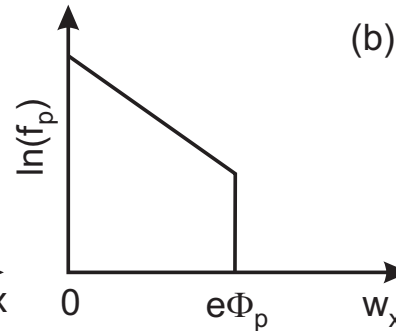
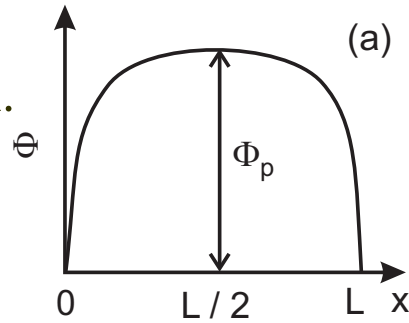
- (a) The penetrated electron beam flux (curve 2) gradually approaches to the emitted flux value (curve 1).
- (b) Initially phase plane ($t = 199 \text{ ns}$) shows the intense permanently existing two-stream instability.
- (c) At the end of simulation ($t = 499 \text{ ns}$) phase plane shows the unperturbed beam.
- (d) Initially ($t=119 \text{ ns}$), the total EVDF (solid line – plasma, dashed line - beam) near the emitting wall ($x=0$) is non-monotonic.
- (e) At the end of simulation ($t = 499 \text{ ns}$), the plateau forms on the plasma EVDF (solid curve), so that **the total EVDF becomes a monotonically decaying function of speed \Rightarrow the instability vanishes.**



The two-stream instability develops when the total EVDF (bulk + emission) is a non-monotonic function.

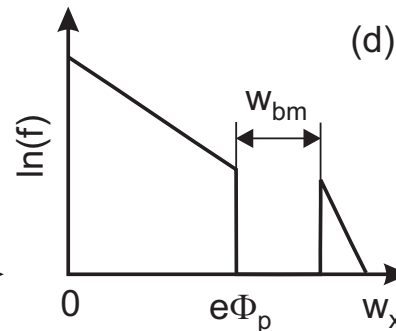
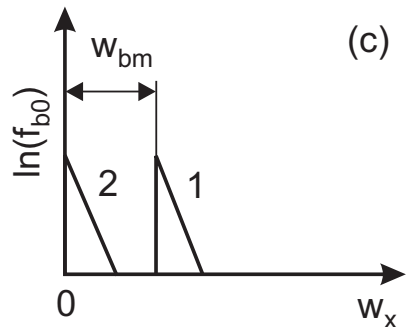
$$\frac{\partial}{\partial(v^2)} f(v) > 0.$$

The potential well.



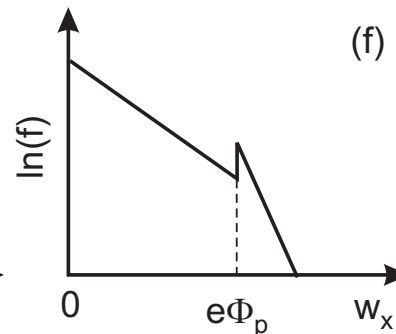
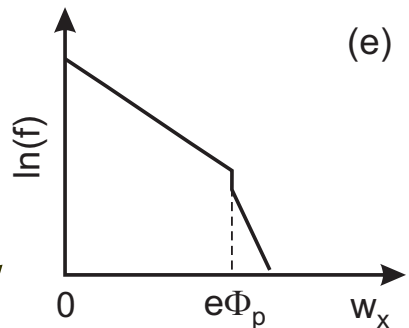
The depleted plasma EVDF.

Possible emission EVDFs: **monotonic (2)** and **non-monotonic (1)**.



Beam + plasma EVDF for **non-monotonic emission EVDF**. *The two-stream instability is expected.*

Beam + plasma EVDF for **monotonic emission EVDF**, low current. *No two-stream instability should occur.*



Beam + plasma EVDF for **monotonic emission EVDF**, high current. *The two-stream instability is expected.*